MOS VOC “air quality” sensors – long-term stability and use for residential ventilation control

Final report

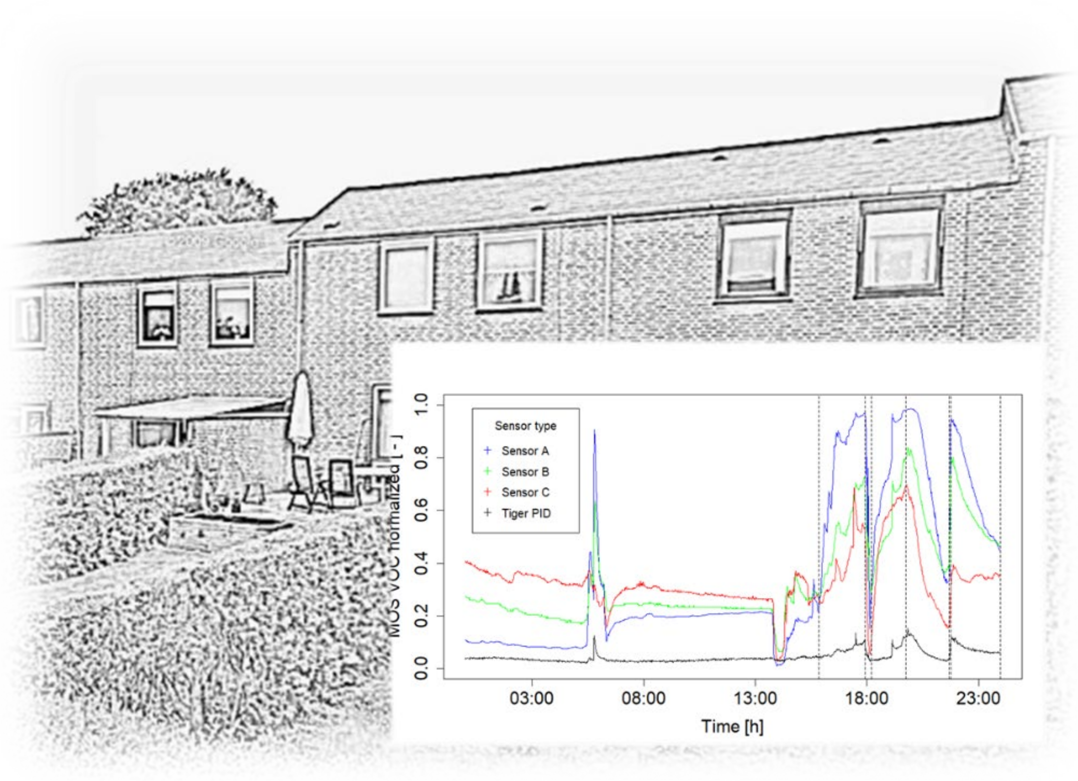

Jakub Kolarik
Section for Energy and Services, DTU Construct
jakol@dtu.dk

The project was supported by Bjarne Saxhofs Fond in the period
October 2020 – December 2023
www.saxhoffondenbyg.dk

MOS VOC "air quality" sensors – long-term stability and use for residential ventilation control
Final report

July 2024

By
Jakub Kolarik, jakol@dtu.dk

Cover photo: Jakub Kolarik
Published by: DTU, Department of Civil and Mechanical Engineering, Brovej, Building 118, 2800 Kongens Lyngby Denmark
www.construct.dtu.dk
ISSN: [0000-0000] (electronic version)
ISBN: [000-00-0000-000-0] (electronic version)

ISSN: [0000-0000] (printed version)
ISBN: [000-00-0000-000-0] (printed version)

Preface

At DTU Construct (earlier DTU BYG), the research related to Metal Oxide Semiconductor (MOS) sensors for measuring Volatile Organic Compounds (VOC) dates back to 2014. Our research and other studies published in the literature have shown that MOS VOC sensors are useful to detect high pollution events such as cleaning, painting, or high occupation density. These abilities make MOS VOC sensors suitable for so-called Smart ventilation systems. According to the Air Infiltration and Ventilation Centre (aivc.org), Smart ventilation is “a process to continually adjust the ventilation system in time, and optionally by location, to provide the desired Indoor Air Quality (IAQ) benefits while minimizing energy consumption, utility bills and other non-IAQ costs (such as thermal discomfort or noise).” MOS VOC sensors express affordable and easily applicable IAQ monitoring and control technology. The commercial landscape of MOS VOC sensors is large. There are dozens of producers offering sensors at various prices and quality. This report summarizes the results of the research project supported by Bjarne Saxhofs Fond between October 2020 and December 2023. The project aimed to evaluate the performance of several commercially available sensors with respect to their application in a common residential environment. The intention was to address the practical issues of their usability, potential drawbacks, and benefits.

This report describes the projects’ results in three parts. The first and most significant part is evaluating sensors deployed in realistic residential environments. The second part describes laboratory experiments, which aimed to test the sensors under exposure to controlled emissions of pollutants, connect the sensors to a ventilation unit, and suggest an algorithm to process their output signals. The third part describes modelling work to estimate energy-related aspects of MOS VOC sensors’ use.

Kgs. Lyngby, July 2024

Content

Summary

Metal Oxide Semiconductor (MOS) sensors measuring Volatile Organic Compounds (VOC) seem to be an obvious step towards broadly available Demand Controlled Ventilation (DCV). Previous research shows that sensors can detect pollution events such as cleaning, painting, or high occupation density. These abilities make the MOS VOC sensors suitable to complement ventilation control systems, especially concerning residential ventilation. Practically, there are still unanswered questions like: “Are the MOS VOC sensors reliable and stable enough to be applied in practice?” “Are there any benefits concerning energy efficiency and indoor environmental quality?” “How to deal with the MOS VOC sensor signal?” The present project focused on exploring the performance of MOS VOC sensors. We aimed to bring answers to the aforementioned questions. The project was comprised of three parts: field measurements, laboratory measurements, and computer simulations.

During the field measurements, we investigated the performance of commercially available MOS VOC sensors exposed to a typical residential environment. We determined their properties – sensitivity, linearity, and hysteresis. We measured in a typical Danish row house occupied by a family of four. We installed two sets of three commercially available sensors in the bedroom and kitchen. Photo Ionization Detector (PID) served as a reference measurement. The field measurements conducted in a real house showed that all tested sensors detected the pollutant emissions in the residence. Two of the sensors had comparable sensitivity. There was also an apparent relationship between their output signals. Statistical analysis employing a cross-correlation function has confirmed this relationship. These sensors would behave similarly when used to control a ventilation system in the house. Several MOS VOC sensors provide so-called CO_2 equivalent signal. This measure is based on a correlation between emissions of pollutants from humans and the metabolic production of CO_2. Our analysis of the relationship between the CO_2 equivalent signal and the actual CO_2 concentration showed, in general, a weak correlation. There were large discrepancies between the two signals in the kitchen where the human bioeffluents were not the main pollution source. The discrepancies in the bedroom were smaller, but the correlation was also weak. Therefore, we conclude that CO_2 equivalent signal should not be used as a surrogate for CO_2 concentrations. Our results indicate that the characteristics of the MOS VOC sensors need to be carefully considered in ventilation control algorithms and that the sensors from different manufacturers need to be considered individually. There is no “one fits all” implementation scenario.

During the second part of the project, we exposed the sensors to controlled emissions of typical residential pollutants in a field laboratory. It comprised a room in a test house at the Technical University of Denmark. It resembled a residence, but we could control the environmental conditions. The field laboratory was equipped with a residential ventilation system providing balanced airflow. The tested sensors were placed in the middle of the room and exposed to controlled emissions (pollution scenarios) of human bioeffluents, window cleaning agent, limonene emissions originating from oranges, and ethanol emission, representing extreme pollution event. We connected one MOS VOC sensor to an external controller to control the ventilation system. The experiments in the field laboratory showed that all tested sensors had rather comparable behavior with respect to the tested pollution scenarios. As it was impossible to connect all tested sensors to the controller, we conducted parallel measurements. Their results

indicate that all sensors reacted similarly to the pollution scenarios. However, the differences in the character of their output signals (e.g., different units expressing concentration or even a preprocessed index indicator) would need to be taken into account during implementation with a concrete controller. During the test in the field laboratory, we developed an algorithm using a running mean with an adjustable k value (representing the length of the time window for signal averaging) to process the MOS VOC signal. The algorithm continuously adapted the k value in response to the actual measured concentration. This allowed the reduction of both peaks in the control signal and the consequent short-term airflow boost. However, the algorithm did not consider the relative nature of the MOS VOC signal. This is highly recommended before its application in practice.

The third part of the project comprised modelling of the ventilation control equipped with MOS VOC sensor. We created a model of the row house used for the field measurements in the simulation tool IDA Indoor Climate and Energy. Our approach was to use data from the field measurements to mimic a realistic VOC emission profile and an occupancy profile. We identified two month period in the measurements (February and March 2022), which was suitable for the modeling. The period included one week of winter vacation, where the house was unoccupied. This provided background concentrations of the VOC signal measured by the MOS VOC sensor. We used the MOS VOC-based CO_2 equivalent signal for modelling. We tuned the simulation model to correspond to the measured data. For this purpose, we simplified the model to three zones on the ground floor- kitchen, living room, and entrance. We simulated a mechanical ventilation system with heat recovery working with constant air volume and controlled by CO_2 and CO_2 equivalent concentration. The simulations showed that using CO2 equivalent concentration for controlling the ventilation system led to higher heating energy consumption (by 16%) and extensive fan electricity use (68%) compared to constant air volume system. This was a consequence of higher ventilation air flows used by the system due to higher fluctuations and generally higher absolute values of the CO_2 equivalent concentrations. Utilization of moving average for the signal processing led to a slight but further increase of energy consumption. The moving average approach decreased the concentration peaks but simultaneously brought prolonged periods with higher concentration levels. The results show that using the MOS VOC signal, the demand controlled ventilation would adjust the airflow more frequently as the VOC signal has higher variability. Further optimization of the control algorithm would be needed to find the balance between indoor air quality and energy consumption.

To answer the practical questions defined in the beginning, we can conclude that two of the tested sensors presented stable and comparable behavior during long-term measurements and laboratory tests. The results of the project do not allow for the direct assessment of indoor air quality benefits, but as the MOS VOC control led to higher airflows, assuming clean outdoor air, the influence would probably be positive. Concerning energy efficiency, our results show that applying MOS VOC sensors would increase energy consumption. Therefore, their application should be motivated to remove unwanted pollutants rather than save energy. As these sensors cannot measure absolute concentrations and provide relative measurements, they are suitable for detecting sudden emission peaks but not for long-term monitoring of background pollutant concentration levels. Therefore, they are unsuitable for monitoring air quality when lowering the background (minimum) ventilation rate, which would otherwise be an apparent energy-saving measure.

1. Introduction and background

Today's energy efficient buildings are airtight and need efficient ventilation to maintain high indoor air quality (IAQ). Smart ventilation (Durier et al. 2018) allows for continuous adjustment of ventilation in time, and location, to provide the desired IAQ while minimizing energy consumption. Smart ventilation finds its way into new or renovated houses, not only in Europe but also in the USA. It is mostly a sub-type of smart ventilation, Demand Controlled Ventilation (DCV) (Guyot et al. 2018), which is becoming increasingly popular even in the residential sector, where we would not expect it to be applied some decades ago. This is primarily due to technological advances in building control (digital and internet-enabled controllers, EC fans) and the development boom with respect to IAQ sensors. Sensors measuring temperature, concentration of CO_2, Volatile Organic Compounds (VOC), or relative humidity are produced cheaply and in compact dimensions. Metal Oxide Semiconductor (MOS) sensors for measuring VOC (Herberger and Ulmer 2012, Schütze et al. 2017) offer a possibility to account for pollution related to human presence and activities as well as other pollution sources. It is their clear advantage. A ventilation system can increase airflow when pollutants from cleaning or cooking are detected. Other advantages of MOS VOC sensors include low energy consumption, small dimensions, and durability. Moreover, Herberger et al. (2010) developed a sensor that uses data collected by Burdack-Freitag et al. (2009) correlating the measured VOC signal with human emission of CO_2. The sensor's output, so-called CO_2 equivalent concentration, expresses the level of pollution. As CO_2 concentration became known to the public as an indicator of IAQ, the intention was for the building occupants to interpret sensor signals more easily and simplify the implementation of the sensors in ventilation systems.

All the above mentioned arguments speak for the MOS VOC sensor technology, and ventilation producers currently offer VOC-controlled DCV for residential applications. At the same time, some studies, like Won and Schleibinger (2011), describe the drawbacks of the technology. They mention a high cross-sensitivity to moisture in the air, low resolution, and inability to measure the concentration of individual chemicals. The body of literature on MOS VOC sensors is extensive and the field is developing very fast. We recommend the work of Chojer et al. (2020) and Gacia et al. (2022) for the recent updates. Recent works successfully addressed some of the limitations mentioned by Won and Schleibinger (2011). However, the solutions are often very far from practical applications. And talking about practice, the studies evaluating the field performance of MOS VOC sensors are not very frequent. Demanega et al. (2021) extensively evaluated low-cost environmental monitors, including MOS VOC sensors in laboratory conditions. They observed a strong correlation of sensor signals with the reference instruments but a poor agreement concerning absolute values of VOC concentrations. Kolarik et al. (2023) applied cluster analysis to compare the behaviour of five commercially available MOS VOC sensors. Their results showed that most of the sensors agreed with the reference measurements. Using cluster analysis showed that the sensors from different manufacturers might react to various pollutants, and thus, their behaviour altered depending on the pollutants in the space. In their field measurements, Kolarik (2014) observed an agreement in the need for increased ventilation expressed consistently by VOC and CO_2 sensors during 49% of occupied time. During 11% of occupied time, only the VOC sensor indicated the need for increased ventilation. This would mean that at 11% of the time, the system would work with higher ventilation than the CO_2 control. One can say that this is the price for higher air quality. Others admit that such an operation would not lead to decreased energy consumption. Also, De Sutter et al. (2017) illustrated challenges related to the direct replacement of CO_2 sensors with MOS VOC sensors. Their results also showed a notable increase in ventilation rates. These were associated with sharp peaks in the MOS VOC signals while the same set point was used for CO_2 and VOC control. The authors suggested a correction algorithm that would filter the VOC signal, but they did not demonstrate its application. Moreno-Rangel et al. (2018) assessed a low-cost IAQ monitor's precision, accuracy, and usability in a residential environment (a bedroom). They observed a significant agreement with the reference instrument. At the same time, the CO_2 equivalent signal from the MOS VOC IAQ monitor was found to provide misleading CO_2 levels as indicators of ventilation. A study by Baur et al. (2021) investigated the potential and limits of MOS VOC sensors and applied calibration with randomized exposure and data-based models trained with advanced machine learning. The study included both laboratory calibration and field testing. In addition to monitoring normal ambient air, the authors conducted pollution release tests with VOCs included in the laboratory calibration. Extensive laboratory-grade measurements were performed in parallel to the MOS VOC measurements. The results showed a quantitative agreement between reference measurements and the MOS VOC sensors. On the application side, Sørensen and Kristensen (2024) applied low-cost sensors, including MOS VOC, to investigate concentrations of CO_2 and VOC in classrooms. The study demonstrated that low-cost sensors were useful for uncovering general trends regarding VOC dynamics. Nevertheless, the MOS VOC sensors were used as an additional monitoring tool, not for the actual ventilation control.

2. Aim and objectives

Aim of the current project was to provide information regarding performance and utilization of commercially available MOS VOC sensors for ventilation control in residential settings. The project was divided into three parts that cover the different aspects of the MOS VOC application. Primarily, we exposed the sensors to realistic residential conditions and determined their characteristics using the measurement data. Consequently, we tested the sensors in a field laboratory. Based on these tests, a ventilation control algorithm was suggested, and its functionality was evaluated. Finally, we performed computer simulations to estimate the influence of MOS VOC based ventilation control on energy consumption for heating and ventilation.

2.1 Performance of MOS VOC censors under real residential conditions

The first part of the project focused on the performance of the MOS VOC sensors under realistic residential conditions. We investigated the sensors' characteristics, normally investigated in laboratory conditions, using data collected in the field. This part had the following objectives:

1. Investigate the long-term performance of MOS VOC sensors exposed to a typical residential environment.
2. Determine sensor properties – sensitivity, linearity, and hysteresis by comparing their signal with a reference measurement.
3. Evaluate the correlation between the CO_2 equivalent signal produced by the MOS VOC sensor and actual CO_2 concentration.

2.2 MOS VOC sensors for control of a ventilation system

The aim of the second part of the project was to investigate the behaviour of the MOS VOC sensors together with a simple residential ventilation system. We conducted the “field laboratory” tests focused on establishing a control algorithm and testing the system's response to different pollutant emissions. The part had the following objectives:

1. Implement MOS VOC sensors in a prototype of ventilation control and demonstrate its functionality.
2. Create a laboratory set-up comprising residential ventilation equipped with a MOS VOC sensor to control the airflow.
3. Set up a controller taking the MOS VOC signal into account and suggest a control algorithm that includes processing the MOS VOC signal.
4. Demonstrate functionality of MOS VOC based control under different pollutant emission scenarios corresponding to indoor environment in residencies.

2.3 Estimating energy-related aspects associated with MOS VOC sensors

The aim of the third part of the project was to determine the effect of MOS VOC based control on energy consumption in the building. We created a simplified model of the residence used in the first part of the project. We used the measured data to estimate the house's occupancy and VOC emissions measured by the MOS sensor. We simulated a balanced mechanical ventilation system with heat recovery controlled according to different strategies, including the MOS VOC signal. The part had the following objectives:

1. Create a numerical model of the residence where the long-term field measurements were conducted.
2. Simulate different scenarios for residential ventilation control.
3. Evaluate energy demand for heating and ventilation as well as the functionality of control scenarios.
4. Compare the energy demand and functionality of ventilation control based on MOS VOC signal with CO_2 based and constant air volume ventilation.

3. Methodology

3.1 Approach

The project was divided into three parts (Figure 1). The first part comprised an evaluation of the sensor's real life performance in a realistic residential environment. We placed the sensors in a typical Danish row house occupied by a family of four (two children and two adults). We conducted the measurements from September 2021 until June 2022. The project's second part involved a laboratory study on a control algorithm involving the MOS VOC sensor. We connected a commercially available residential air handling unit to a modular controller receiving a MOS VOC sensor signal. We investigated several strategies for processing the sensor signal. The third part comprised building simulation modelling. We created a model of the row house and used the measurement data to tune the model to represent the building. Consequently, we simulated different ventilation strategies, including ventilation controlled by MOS VOC sensor. We evaluated the performance of the strategies regarding heating demand and electricity use.

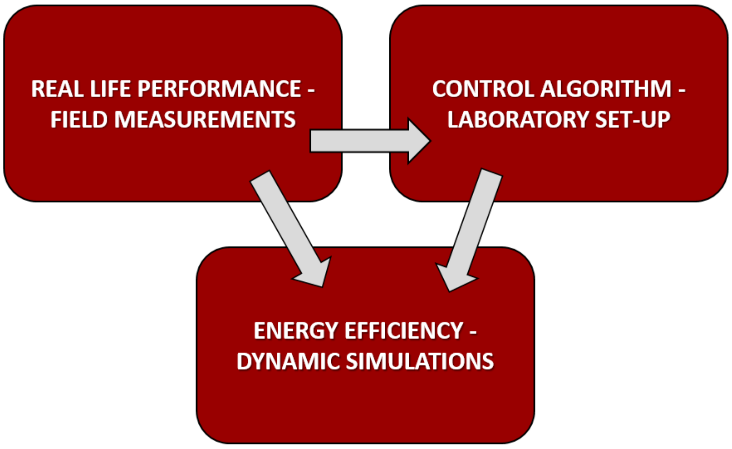

Figure 1 – Structure of the project

The following sections describe the methodology used in particular parts of the project.

3.2 Measurements in real residential environment

3.2.1 Tested commercial sensors

We based the choice of the sensors on the results from a previous national project (Kolarik et al. 2018). Additionally, the choice was driven by our intention to test sensors offering different ways to interpret the output. We selected sensors with an analogue output, an output representing CO2 equivalent concentration, and an output processed into a custom IAQ indicator. Table 1 summarizes the technical parameters of tested sensors. We investigated three different sensors. We purchased two specimens of each sensor and created two measuring sets. We integrated the sensors into one casing with a combined power supply. We used the Arduino board with Wi-Fi module for wireless signal transfer. We stored the data on a laptop PC. We used a portable photo-ionization (PID) gas detector, Photo Check TIGER, for reference measurements. As the PID technology does not allow for selective measurements of particular VOCs, we abbreviate the signal provided by the PID instrument as $TVOC_{PID}$. We adopted the Salthammer (2022) approach, which indicated that the PID instrument measured the sum of VOC. Before the measurements, we performed a custom calibration of the PID gas detector with 100 ppm of isobutylene (zeroing on zero gas mixture). The $TVOC_{PID}$ concentrations thus represented isobutylene equivalents. The instrument had a detectable range of 1 ppb-20,000 ppm (minimum resolution 1 ppb or 0.001 mg/m^3 isobutylene at 20 °C and 1000 mBar) and accuracy ± 5 % of a display reading. Besides the MOS VOC signals, we also monitored standard indoor environmental quality (IEQ) parameters: room temperature (±0.3 °C 5-60 °C), relative humidity (±2 % RH 20-80 % RH), and CO_2 concentration (non-dispersive infrared-NDIR, 400-2000 ppm, ±30ppm ±3 % of reading). We used internet-connected commercial indoor climate monitors providing measurements in 5-minute intervals. In comparing MOS VOC signals and the IEQ variables, we averaged the 1-min MOS VOC data into 5-min intervals.

Table 1 – Technical parameters of investigated sensors (according to manufacturer data)

Abbreviation	**A**	**B**	**C**
Type	SGP40	EM 8100	CCS811
Manufacturer	Sensirion A.G.	Figaro Engineering Inc.	ScioSense B.V.
Output (units)	VOC index [-] [(a)]	Voltage [V]	$TVOC_{MOS}$ eq. [ppb][(b)] CO_2 eq. [ppm]
Sensing range	0÷500 VOC index points; 0÷1000 ppm ethanol equivalents	0-3.0 V DC; 1-30 ppm H_2	0÷29206 ppb $TVOC_{MOS}$ eq. 400÷32768 ppm CO_2 eq.
Measuring accuracy	± 15 VOC index points	N/A	N/A
Measurement interval/ response time	N/A/ < 10 s	N/A	N/A
Power Supply	1.7-3.6 V DC	4.9-5.1 V DC	1.8-3.6 V DC
Communication	I^2C bus	0 – 3.0 V DC	I^2C bus
Warm-up time	N/A	N/A	20 min
Operation temperature range	-20÷55 °C	-10÷50 °C	-40÷85 °C
Operation humidity range	0÷80 %, non-condensing	NA	10÷95 %, non-condensing

(a) A built-in proprietary algorithm processes a raw sensor signal to obtain the VOC Index. The scale does not represent absolute concentrations.

(b) The sensor processes the raw signal into a VOC sum $TVOC_{MOS}$ and CO_2 equivalents. The algorithm for CO_2 equivalents is proprietary; the manufacturer states that CO_2 equivalents are determined based on the relationship between human production of VOC (bioeffluents) and CO_2.

3.2.2 Data processing

As each studied sensor provided a different output signal, we normalized these signals to avoid the influence of the absolute value of each observation. Each observation was normalized against the difference of its maximum value and minimum value, as shown in Equation (1):

$$y = (x - \min(x))/(\max(x) - \min(x)) \qquad (1)$$

Where *x* is the i-th observation in the measured data and *y* is the i-th normalized observation for the particular sensor signal. We used only the normalized data in our analyses.

We used so-called characteristic curve to describe the sensor properties. Fahlen et al. (1992) determined the curve by exposing the sensor to a set of steady-state concentrations of a known VOC in ascending and descending order. In the present paper, we established the characteristic curve by fitting the linear regression model to the data with PID measurements as independent and MOS VOC data as dependent variables. The slope of the relationship represented the sensor's sensitivity. The R^2 value for the linear model indicated the linearity of the sensor. To evaluate hysteresis, we selected one-day measurements from the data. We fitted a linear regression model to build-up and decay periods separately. Consequently, we expressed the hysteresis as a mean distance from the two regression lines. We used the obtained linear models to determine such distance to predict the MOS VOC signal for three distinct reference signal levels (150 ppb, 250 ppb, and 350 ppb isobutylene equivalent). The mean difference between such predictions for build-up and decay determined the hysteresis.

We applied Justo Alonso et al. (2021) approach to determine a correlation among the signals from tested MOS VOC sensors and a correlation between the CO_2 equivalent signal provided by sensor C and the absolute CO_2 measurements by the NDIR sensor. We used a cross-correlation function (CCF) to calculate a correlation between two time series (sensor measurements), considering different time lags (Madsen 2007). The result of such analysis is the CCF plot depicting the correlation between the studied time series in so-called time lags. Pearson's coefficient in the particular time lag represents the correlation. Correlation in time lag zero indicates that the studied variables change simultaneously. The correlation in higher time lags suggests that the change of the first variable precedes the change of the second.

3.2.3 The test site row house and the measurement period

We have installed the senor sets in a typical Danish row house occupied by a family of two adults and two children (elementary school age). We placed the sensor sets in two locations- a kitchen/dining room open to a living room and the main bedroom (Figure 2). The Figure 3 depicts the installation of the MOS VOC sensors, IEQ monitor and the reference measurement PID device in the bedroom of the row house.

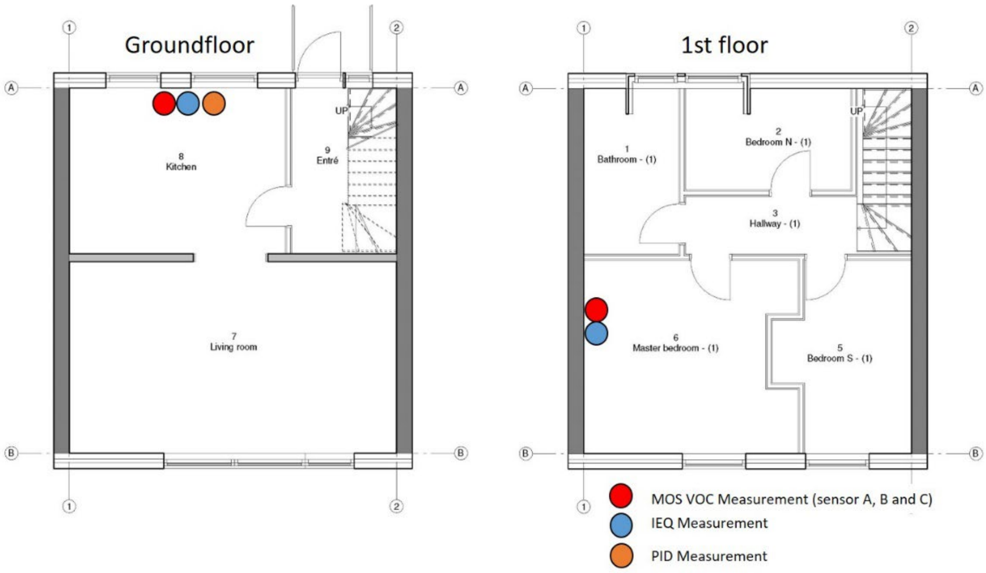

Figure 2: Placement of the sensors during field measurements in the row house

The measurements lasted from September 2021 until June 2022. However, we do not present all the data in this report. During the data quality assessment, we disregarded some data because of errors, such as a disconnected power supply, wrong measurements because of technical problems, etc. Moreover, despite the original plan, conducting the PID measurements continuously during the whole measurement period was impossible. The device was noisy when in operation, disregarding the possibility of measuring in the bedroom. The noise was simply to disturbing for the occupants, even if the device was placed in the corridor. Also, for the measurements in the kitchen, the PID measurements were not possible for a whole period. Therefore, we screened the data to identify suitable periods for analysis. This report includes measurements from September-November 2021 and February-March 2022. Furthermore, we identified specific weeks and days and used them for detailed analysis.

Figure 3 – Installation of the MOS VOC sensors in the bedroom

3.3 MOS VOC sensors for ventilation control – laboratory measurements

3.3.1 The “field laboratory”

We conducted the tests in the field laboratory situated at the Technical University of Denmark. The term “field laboratory” means the premises where the experimenter has the possibility to adjust the environmental conditions, but at the same time, the space has the characteristics of a real built environment. Figure 4 illustrates the view and setup in the field laboratory. The room's window was oriented to the north-northeast; its dimensions were 2 m x 1.3 m. The volume of the room was 25.4 m^3 (3.5 m x 2.9 m x 2.5 m). In addition to the ventilation unit and the controller, the room contained two desks, three chairs, an electric heater, an ultrasonic air humidifier, and a laptop computer with a docking station. Smaller walls (2.9 m x 2.5 m) were lined with wooden boards, the larger walls (3.5 m x 2.5 m) and the ceiling were made of plasterboard. The floor was covered with linoleum. We conducted measurements of infiltration to judge the air tightness. The mean infiltration was 0,4 h^{-1}, corresponding to 0,27 $L/s \cdot m^2$.

Figure 4 – Left: a view of the field laboratory, right: residential air handling unit

3.3.2 Air handling unit

Swegon CASA W3 Smart air handling unit was used as a representative system for residential ventilation (Figure 4-right). It is a compact air handling unit with heat recovery and an electric reheat coil. The unit is equipped by two 230 W fans having an operating range of 36 m^3/h to 288 m^3/h. The unit was connected to ductwork, which represented simplified ductwork in a residence. There was one supply and one exhaust diffuser. Each part of the ductwork was equipped by adjustable dampers. The unit can be operated in different control modes as well as controlled by an external controller. We used an external controller to determine a MOS VOC control algorithm and test the signal processing. The manual control using the wall mounted control panel included three modes: Away (basic ventilation in unoccupied residence), Home (ventilation under occupancy) and Boost (increased ventilation in the case of cooking etc.). The unit was commissioned to provide certain levels of constant airflow in the particular operation modes. These were: Away – 34.7±1.0 m^3/h, Home – 49.7±1.4 m^3/h and Boost – 120.3±2,5 m^3/h. The values represent mean ± standard deviation from the commissioning measurements.

Additionally, the unit can operate according to several automatic control algorithms, depending on the accessories installed. The unit used in the project was equipped with an MOS VOC sensor (provided by the unit's manufacturer, but the technical data for the sensor are unknown). We compared the built-in control algorithm utilizing the MOS VOC sensor provided by the manufacturer to the developed algorithm. The airflow control has two modes: step based and step less (continuous). The step mode switches between operational modes. We utilized the step less airflow control in the project. The controller provided an output signal within a range from 1 V to 8 V. The maximum control signal of 10 V was utilized to indicate the stop of the unit's operation, while the control signal of 0 V indicated disabled control.

3.3.3 External controller

We used the Loxone miniserver (Figure 5) and the Loxone Config software as an external controller. We designed the software's control algorithm and transferred it to the controller. The miniserver enables connecting various devices and sensors, creating automation scenes and programming different functions and responses. We connected the miniserver to the external input of the air handling unit. The MOS VOC sensor used for control was connected directly to the analogue input of the miniserver.

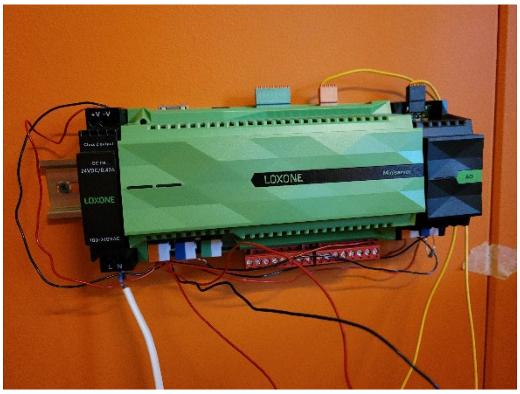

Figure 5 – Loxon miniserver was used as an external controller

3.3.4 MOS VOC sensor connected to the air handling unit

Integrating the MOS VOC sensors tested in the real residential settings (sensor A, B and C, see section 3.2 and Table 1) was not possible as the project budget did not allow for integrating their digital interface to the Loxon miniserver controller. Therefore, we used a MOS VOC sensor RLQ -W by S+S Regeltechnik GMBH (Figure 6 – MOS VOC sensor used for air handling control) to control the air handling unit. The sensor had an analogue output (0-10 V), and could directly connect to the controller. The RLQ -W sensor had an automatic calibration, which automatically adjusted the sensor's baseline to the lowest measured concentration. No re-calibration of the sensor was performed. All sensors were operated continuously in the field laboratory so that their auto calibration algorithms adjusted to the same conditions.

Figure 6 – MOS VOC sensor used for air handling control

3.3.5 Control algorithm and testing procedure

We based the algorithms used for MOS VOC sensor signal processing on the moving average of the raw signal. The main advantage of a moving average is primarily its ability to remove short-term fluctuations in the data and rather follow the developing of long-term trends of the signal. Based on the available literature (for example De Sutter et al. 2017), the high fluctuations in the amplitude of the MOS VOC signal lead to instable control. Among the limitations of this algorithm is the fact that excessive insensitivity can occur if the moving average calculation time window is chosen too large. On the other hand, the low efficiency if the moving average is calculated from a time window that is too narrow. In the tests performed, our goal was to determine the optimal length of the interval-number of previous data points for calculating the moving average, so called k-value. We tested fixed values of 3, 5, 10 and 15 minutes. Additionally we developed an algorithm with adaptable k-value. This algorithm adjusted continuously the amount of previous data points (concentration values) included in the moving average, based on the actual measured concentration level. The linear function was used to describe the relationship between actual concentration and the k-value (Figure 7).

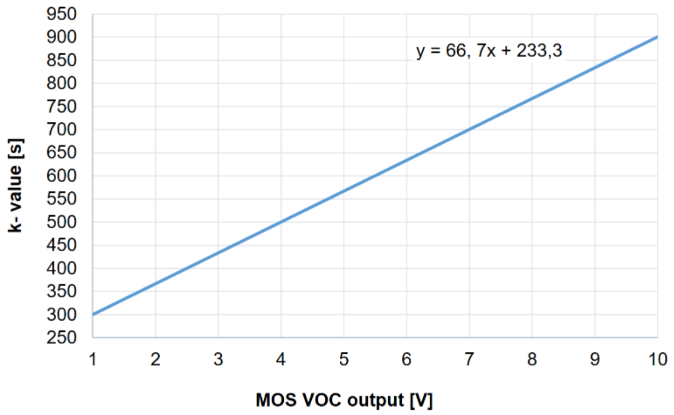

Figure 7 – Relationship between the k-value and actual MOS VOC sensor signal

The Figure 8 illustrates the block diagrams for the particular control algorithms as implemented in the Loxone Config software. The first diagram from the top is the connection for the unprocessed signal. The intermediate scheme is a moving average implementation with a constant time interval (3 minutes, 5 minutes, 10 minutes and 15 minutes). The last, bottommost, diagram is a block diagram implementing the last algorithm, a moving average with a variable time interval length. In the "Formula" block V1, the equation from Figure 7 was implemented.

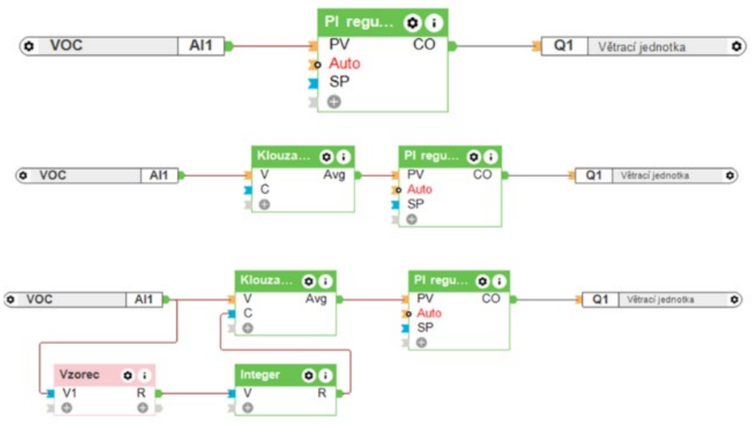

Figure 8 – Implementation of the control algorithms in then Loxone Config software

3.3.6 Testing the control algorithm

We conducted two evaluation campaigns in the field laboratory. The first series of tests (further called “Test campaign 1”) was conducted in parallel with the development of the control algorithm. This tests included only signal from the MOS VOC sensor connected to the air handling unit. The second series of tests (further called “Test campaign 2”) followed consequently and included signals from other tested sensors (for their description, see section 3.2).

Test campaign 1

The aim of the procedure was to achieve distinct air pollution levels in the test laboratory and thus verify the functionality of the control. We selected the pollution sources to represent residential VOC emissions (see Kolarik et al. 2023). The procedure was the same for each measurement day so that the data were mutually comparable and we carried all activities mentioned below with an accuracy of ±5 minutes. The procedure is summarized in Table 2.

Table 2 – Test campaign 1- pollution scenarios

Time of day	Pollution scenario	Additional information
min. 12 h prior to the experiment	Empty field laboratory - background	The air handling unit set to external control, min. airflow adjusted at 60 m^3/h
8:30	One adult human subject entered the field lab.	Human bioeffluent emission.
9:00	Painting with an alcohol based marker – A square (10 cm x 10 cm) was drawn on paper. The painted paper was left on the table for 10 minutes, and finally taken out of the room.	Emission of ethanol, xylene, butanol – based on the manufacturer information.
10:30	Peeling an orange. The peels were left on the table for 10 minutes, and finally taken out of the room.	Emission of aromatic substances e.g. terpenes, pinenes or limonenes (Pinheiro et al. 2018)
12:00	Utilization of perfume spray (4-5 doses). The perfume was sprayed freely into the room.	Emission of oxybenzene and tetramethylhydroxypiperidinol – based on the manufacturer information.
14:00	Window cleaning The window was sprayed evenly with 10 doses of a commercial cleaning agent, which were wiped off with a dry cloth after 3 minutes. The process was repeated 5 times.	Emission of limonene, ethanol and acetone – based on the manufacturer information.
15:45	Hand disinfection – one dose of hand disinfection, then waiting for about 5 minutes to dry.	Emission of ethanol and isopropanol – based on the manufacturer information.
16:00	The human subject leaves the field lab. End of test.	

Test campaign 2

The second round of tests focused on the behaviour of all tested sensors (see Table 1 and section 3.3.4). Additionally, we tested also the functionality of the control algorithms- the one developed within the project and the embedded algorithm in the air handling unit. In addition, we conducted reference measurements with a PID air quality monitor (for description of the instrument see section 3.2.1). We used Two types of pollution scenarios. The first scenario included a human presence as well as a sequence of pollution events typical for residential environment- peeling an orange (A), window cleaning (B) with a spray detergent, use of an alcohol based hand sanitizer(C) (for details see Table 3). The second scenario comprised one exposure to ethanol emission without human presence. This scenario represented a rather extreme pollution event. We aimed to excite the MOS VOC sensors to the maximum and observe a consequent development of their signals.

Table 3 – Test campaign 2- pollution scenarios

Time of day	Pollution scenario	Additional information
min. 12 h prior to the experiment	Empty field laboratory- background	All MOS VOC sensors and the PID measurement started
Pollution Scenario 1		
9:15 Exposure E	One adult human subject entered the field lab.	
12:00 Exposure A Peeling an orange	Peeling an orange. The peels were left on the table for 10 minutes, and finally taken out of the room.	
13:15 Exposure B Window cleaning	Window cleaning The window was sprayed evenly with 10 doses of a commercial cleaning agent, which were wiped off with a dry cloth after 3 minutes. The process was repeated 5 times.	
14:15 Exposure C Hand sanitizer	Hand disinfection – one dose of hand disinfection, then waiting for about 5 minutes to dry.	
Pollution Scenario 2		
7:30	5 ml of 93% ethanol was poured into a Petri dish and placed it in the room to allow for evaporation.	

3.4 Modelling energy consumption

3.4.1 Approach to modelling

The aim of the modelling work was to demonstrate the effects of MOS VOC based control on ventilation systems and energy consumption in the residence. We created a model of the row house in the dynamic building simulation tool IDA ICE 4.8 SP2 (Equa 2024). The model corresponded to the building where we used for the long-term measurements (see section 3.2). The modelling work was comprised of reproducing the conditions that we measured in the real building using the simulation model. Even though we first created the model of the whole building, we decided to conduct the simulations on a simplified model comprising three zones on the ground floor (kitchen, living room and the entrance).This was mainly due to the complexity of matching the whole building model with the data measured in the real house.

The IDA ICE is a typical building performance simulation tool that does not allow the simulation of multiple air pollutants. Therefore, we utilized CO_2 modelled by the tool as a surrogate for the VOC concentration in the model. This simplification assumes neglecting the adsorption and resorption of the VOCs on surfaces. As the study aimed to determine energy consumption in the house with the ventilation system controlled by the MOS VOC sensor and not the health effects of the VOC concentrations per se, such simplification was possible.

The modelling procedure was the following:

1. Determine a representative period from the measurement data to be used in all simulations.
2. Determine a realistic occupancy pattern using CO_2 measurements from the test site. Adjust the number of occupants in the respective zones to fit the measured CO_2 concentration pattern.
3. Determine the emission of VOC using the MOS VOC measurements from the test site. Use CO_2 as a marker for the MOS VOC determined emissions. Set the outdoor concentration of CO_2 to a negligibly small value (assumption of clean outdoor air). Modulate the internal CO_2 source to match the measured MOS VOC concentrations and generate a hypothetical VOC emission pattern.
4. Simulate the test building utilizing different types of ventilation control. Analyse energy consumption for heating and ventilation and mechanical ventilation airflows.

3.4.2 Building model

We created a detailed model of the row house located in Kgs. Lyngby, Denmark, built in 1960. The total area of the house is 100 m^2 spread over two levels, with an associated heated basement of 50 m^2. The Figure 9 shows the whole building model.

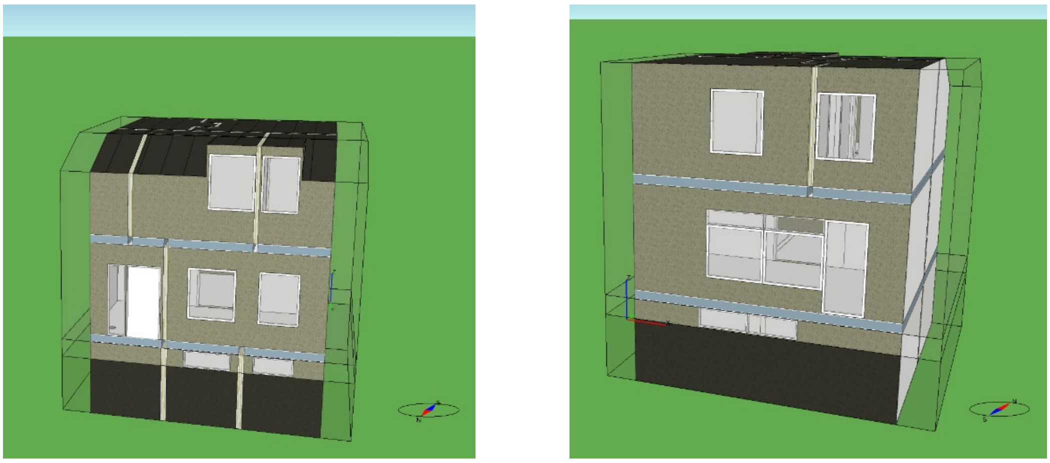

Figure 9 – The whole building model in the IDA ICE simulation tool

Figure 10 presents the simplified 3-zone model. The figure shows the horizontal cross section through the model indicating position of the living room, kitchen and entrance.

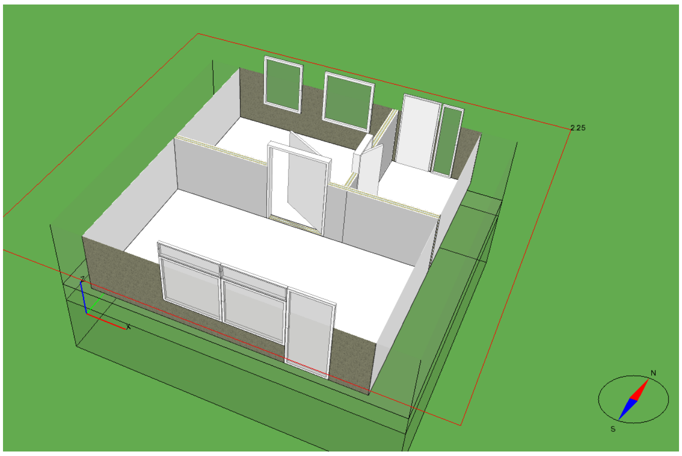

Figure 10 – Simplified 3-zone model used for the simulations

The following description of input parameters relates to the whole building model, however, it is also valid for the simplified 3-zone model. Tables Table 4 and Table 5 summarize the parameters of the building constructions and windows. We determined the parameters based upon technical inspections in the house as well as information from the house residents. Additionally, we utilized information regarding older building constructions available for Danish energy consultants through (Energistyrelsen 2024).

Table 4 - Building constructions used in the simulation model

Construction	Description	U-value [W/m²K]	Dimension [m]	Area [m²]
External wall (façade)	brick wall with air gap (108-74-108 mm)	1.23	0.290	55.33
External wall (basement)	concrete	1.24	0.345	47.62
Dormer wall	timber wall and 50 mm polystyrene isolation	0.69	0.073	1.50
Dormer roof	timber wall – 50 mm mineral wool	0.70	0.073	3.89
Roof	wooden beams and 145 mm mineral wool	0.29	0.174	36.00

Table 5- Windows in the simulation model

Zone	Amount [pieces]	Frame fraction	U-value glazing [W/m²K]	U-value frame [W/m²K]	U-value window [W/m²K]
Kitchen	2	0.15	2.8	2.7	2.785
Entrance	1	0.15	2.8	2.7	2.785
Bedroom North	1	0.15	2.8	2.7	2.785
Bathroom	1	0.15	2.8	2.7	2.785
Tech-room (basement)	1	0.15	5.8	4.5	5.605
Bathroom (basement)	1	0.15	5.8	4.5	5.605
Office-room (basement)	2	0.15	5.8	4.5	5.605

Master-bedroom	1	0.15	1.6	2	1.66
Bedroom South	1	0.15	1.6	2	1.66
Living room	5	0.15	1	2	1.5

We estimated internal loads including heat and moisture production as well as their distribution in time, based on technical visit in the test site house and interview with the owners. Table 6 summarizes the settings of internal loads including electrical appliances and moisture production.

Table 6 - Internal loads and moisture production

Zone	**Number of units [-]**	**Geat gain [W]**	**Operation status**	**Moisture production [kg/s]**
Tech-room (basement)	0.60	45	Always on	-
Office-room (basement)	2.00	200	Schedule	-
Bathroom (basement)	2.65	1294	Schedule	$2.6 \cdot 10^{-4}$
Entrance (basement)	-	-	-	-
Kitchen	4.00	2745	Schedule	$1.1 \cdot 10^{-4}$
Living room	3.00	600	Schedule	-
Entrance	-	-	-	-
Bathroom	1.00	30	Schedule	$2.6 \cdot 10^{-4}$
Bedroom North	1.50	150	Schedule	-
Master bedroom	1.00	75	Schedule	-
Bedroom South	1.50	150	Schedule	-
Corridor	-	-	-	-
Staircase	-	-	-	-

The infiltration in all models was set to wind driven infiltration with air tightness of 0.5 h^{-1} @50Pa. This corresponded to average infiltration of 3.8 L/s in the kitchen and 5.7 L/s in the living room over the simulated period.

3.4.3 Mechanical ventilation systems and heating

We assumed that the row house would be equipped by a balanced mechanical ventilation system with heat recovery (MVHR). In the 3-zone model, we placed the air supply in the living room and the exhaust in the kitchen. We studied three different control strategies for the MVHR system. MVHR CAV control strategy provided balanced airflow corresponding to 0.3 $L/s \cdot m^2$. Additionally, when the kitchen extraction was in operation, the system provided needed make up air. The maximum extracted flow was 65 L/s. The second ventilation strategy was a demand control strategy where the ventilation system was controlled using CO_2 concentration in the kitchen-MVHR DCV. The set-point for the CO_2 concentration was 800 ppm. The airflow range was the same as for MVHR CAV case. The third modelled system was the same as MVHR DCV, but the MOS VOC CO_2 equivalent expressed the ventilation demand- MVHR DCV_{VOC}. In this system, the set-point was 800 ppm CO_2 equivalents. We have also simulated a control algorithm using MOS VOC CO_2 equivalent adjusted using moving average with k = 15 min. See summary of simulated case in the Table 7.

The air handling unit had a specific fan power (SFP) 1000 J/m^3 and a heat recovery efficiency 80%. The supply temperature set point was 18 °C, and there was a water-based heating coil to heat the air in case the heat recovery could not provide the desired supply temperature. The zones were equipped with idealized heaters with unlimited capacity working with the minimum temperature set point of 20 °C.

Table 7 – Simulated types of ventilation system and control

Case abbreviation	Description
MVHR CAV	3-zone model MVHR ventilation continuously at 0.3 L/s·m^2, daily kitchen extract boost (18:00-19:00) at maximum 65 L/s (5 L/s·m^2).
MVHR DCV	Model with MVHR DCV controlled by CO_2 C_{set} = 800 ppm
MVHR DCV_{VOC}	Model with MVHR DCV controlled by CO_{2eq} $C_{MOSVOCset}$ = 800 ppm
MVHR $DCV_{MA,\ k=15}$	Model with MVHR DCV controlled by CO_{2eq} $C_{MOSVOCset}$ = 800 ppm, measured VOC signal processed to provide moving average with k = 15 min

3.4.4 Modelling period

Based on the analysis of the data obtained during measurements in real house, we have selected a period 2.2. - 31.3.2022. This period included one week without occupancy (the house was empty due to winter vacation), thus it gave information about background concentration not directly related to the occupant activities. We utilized the CO_2 and the CO_2 equivalent signals (MOS VOC). Figure 11 shows the measured signals for the chosen period. The CO_2 concentration follows the outdoor concentration during the week of winter vacation. However, the CO_2 equivalent increased for a certain period despite the house being empty. It was not possible to determine the reason for his increase.

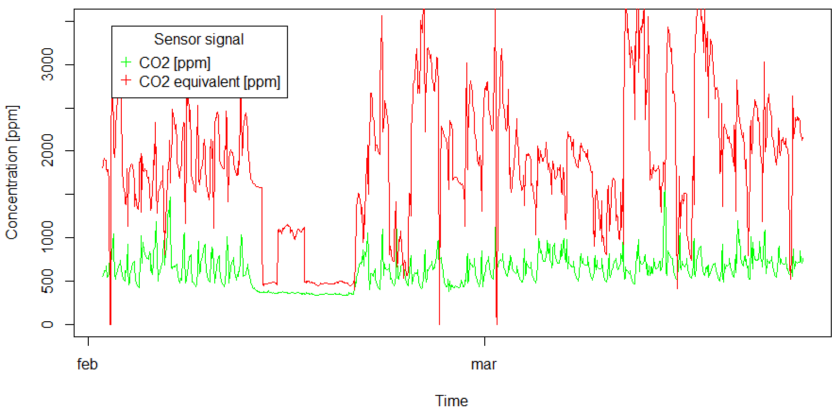

Figure 11 - Measured sensor signals- CO_2 and MOS VOC CO_2 equivalent for the period used in the modelling

3.4.5 User behaviour, occupancy schedule and weather data

The interview with the row house owners provided information about the family's habits and daily routines in a rough outline. The owners were aware of the home's indoor climate, which meant the family regularly ventilated using windows on all floors. The windows opened before the family went to bed in the bedrooms and were left open all night. This behaviour continued generally for the whole year, however, with the addition that if the outside temperature was below 5 °C, then the windows closed at night. We took this into account in the whole building model. The CO_2 concentrations measured in the kitchen during the long term measurements (see section 3.2) served as a basis to determine the occupancy of the space. We conducted simulations using 3-zone model, where the number of occupants in the space was modulated so that the CO_2 concentration in the model corresponded with the measured values. This resulted in the realistic occupancy schedule. Figure 12 presents one week of the schedule.

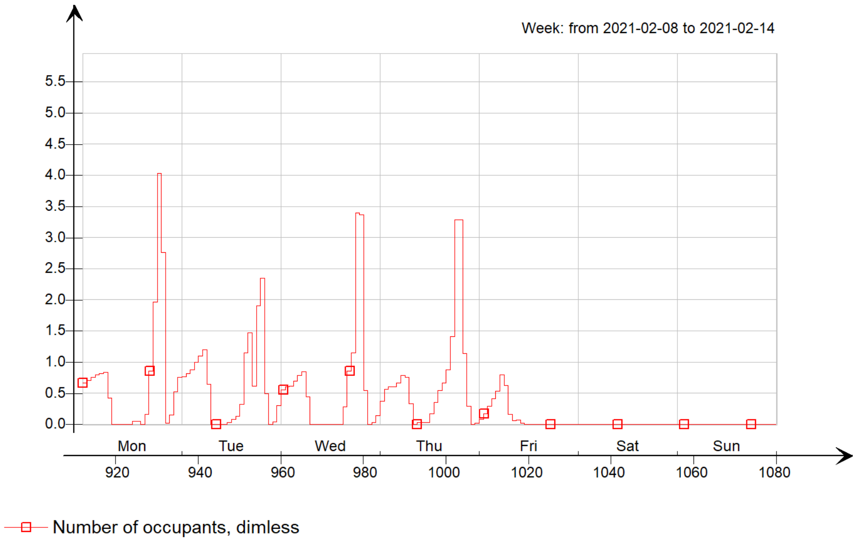

Figure 12 – Occupancy schedule generated using real measurements; example of one week where the family leaves for vacation on Friday

We utilized the same occupancy schedule in all simulations.

Weather data and energy consumption

The Danish Design Reference Year (DRY) (Wang et al. 2013) was used for all the simulations. The weather file is based on data from Danish Weather Authority (DMI) for the period 2001-2010. We applied the primary energy factors according to Danish Building Regulations (BR18 2024). These factors for district heating and electricity were 0.85 and 1.9, respectively.

3.4.6 Determining the VOC source

We used measurements of MOS VOC CO_2 equivalent concentration to determine the hypothetical VOC emission in the space. We were not able to determine the actual emission of VOCs in the row house that could be directly correlated to the CO_2 equivalent concentration. Therefore, we used the measured CO_2 equivalent concentration in the simulation model and while making several assumptions, adjusted a CO_2 source in the model (CO_2 source in the model served as a surrogate of the VOC emission), to reach the same concentrations as measured. The assumptions we made were the following. Infiltration of 0.5 h^{-1} @ 50 Pa and use of a kitchen extract was limited to one hour from 18:00 to 19:00 every day. We considered negligible VOC concentration outdoors. All emissions of VOC registered as CO_2 equivalents took place in the kitchen. The emission rates were dependent on neither air temperature nor relative humidity. There was no sorption and/or desorption of the pollutants on surfaces. In the models considering VOC emissions, we disabled the CO_2 emission from the occupants. This was because the bioeffluent emission was already included in the measured MOS VOC CO_2 equivalent data. Figure 13 gives an example of VOC emission that was determined over one week.

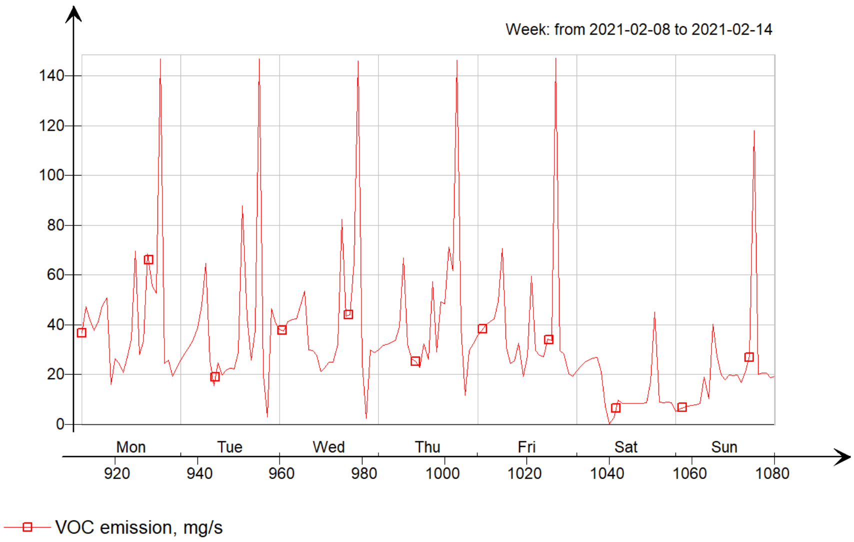

Figure 13 - Hypothetical VOC emission determined from the measured data for MOS VOC CO_2 equivalent concentration

4. Results

4.1 Measurements in real residential environment

We present the data for two weeks in October 2021 to illustrate the variability of measured MOS VOC signals (Figure 14). It depicts non-normalized sensor signals from the kitchen. The figure illustrates a typical signal variability when the row house was empty and occupied. There is a clear difference in the signal amplitude regardless of the sensor type.

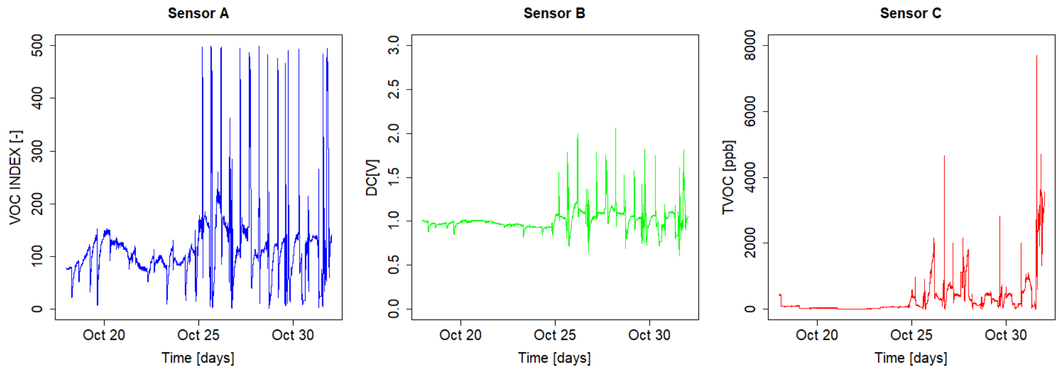

Figure 14: Raw signal of the tested MOS VOC sensors placed in the kitchen; two weeks in October 2021

Figure 15 shows normalized data for the same period as Figure 14. Even though the trend in amplitude of the signals was the same for empty and occupied house, there was a clear difference in the character of the signal. The signal from sensor C was almost zero when the house was empty. On the contrary, signals from sensors A and B had some development, and despite the difference in amplitude of the build-ups and delays, there was an agreement between these two signals. During the occupancy period, sensor A had the largest fluctuations.

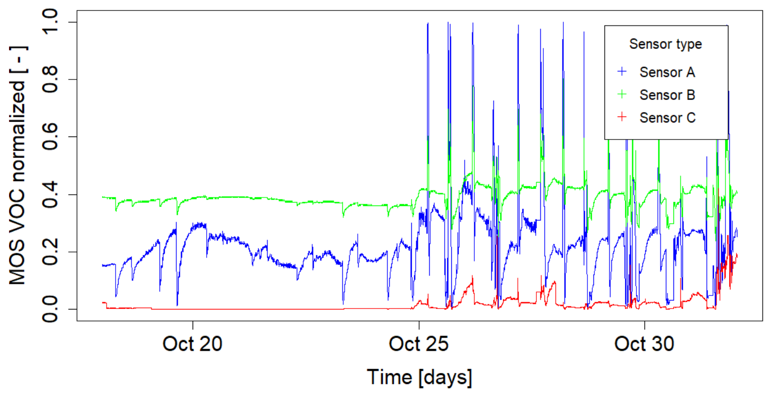

Figure 15 – Normalized signals of the tested MOS VOC sensors placed in the kitchen; two weeks in October 2021

Figure 16 shows a cross plot of normalized signals for the same period. There was a somewhat consistent relationship between sensor A and B responses. The relationship was much weaker when comparing sensors A and B with sensor C. The figure shows only two weeks, but the patterns were similar throughout the analysed period.

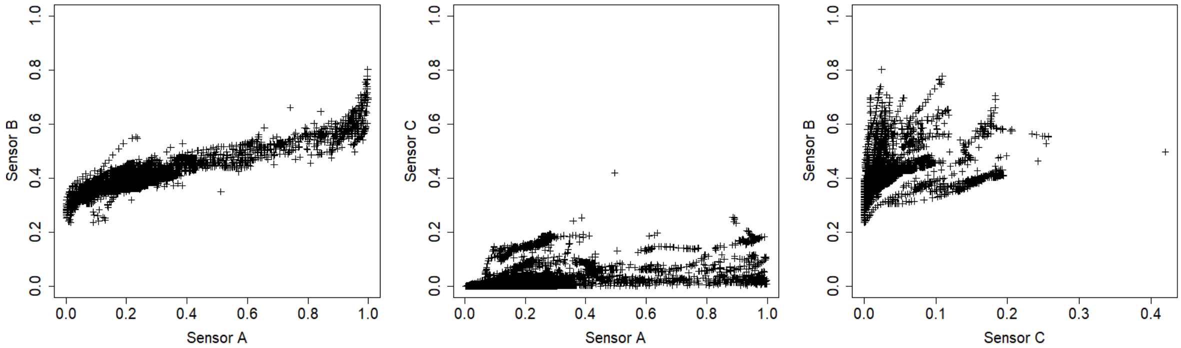

Figure 16 – Cross-plot of normalized MOS VOC signals; two weeks in October 2021

4.1.1 Sensor characteristics

Figure 17 represents characteristic curves determined using measurements from 7.3.2022 until 12.3.2022. We selected this period because it contained consistent and undisturbed $TVOC_{PID}$ measurements. The figure depicts the linear regression fit to the data in the case of sensor A (blue) and sensor B (green). In the case of sensor C, the variance explained by the linear model was too low to consider the linear relationship between the sensor C signal and the reference $TVOC_{PID}$ signal. Table 8 shows the sensitivity and variance explained (R^2) values. We can see from the table and Figure 17 that the response of sensor C did not show any meaningful relation to the PID reference signal. Therefore, sensor C did not seem to represent the changes in the IAQ during the analysed period.

Table 8 – Sensitivity and linearity of the tested sensors

Sensor	Sensitivity (95% conf. int.)[(a)]	$R^{2(b)}$
Sensor A	$2.497 \cdot 10^{-03}$ ($2.432 \cdot 10^{-03}$, $2.562 \cdot 10^{-03}$)	0.40
Sensor B	$1.383 \cdot 10^{-03}$ ($1.350 \cdot 10^{-03}$, $1.416 \cdot 10^{-03}$)	0.44
Sensor C	$7.413 \cdot 10^{-05}$ ($2.042 \cdot 10^{-05}$, $12.78\ 10^{-05}$)	0.0007

(a) The sensitivity- determined as a slope of the linear fit between the MOS VOC sensor signal and the reference signal ($TVOC_{PID}$).

(b) The variance explained (R^2) of the linear fit between the MOS VOC sensor signal, and the reference signal ($TVOC_{PID}$) determined the linearity of the MOS VOC sensors.

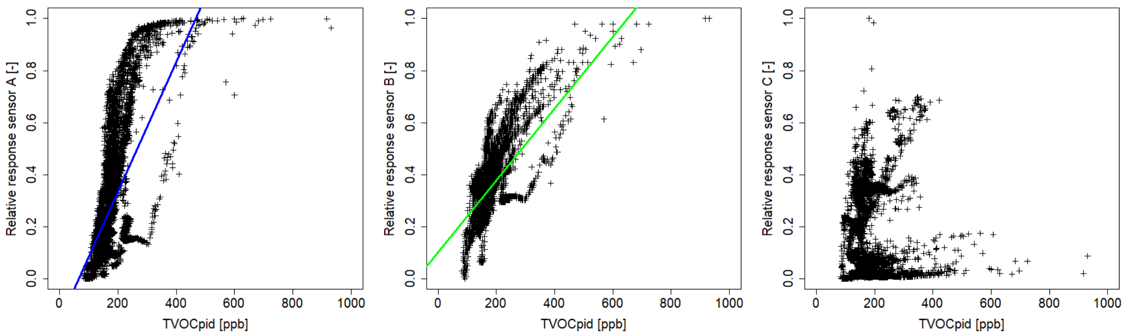

Figure 17 – Characteristic curves for tested sensors

We conducted the analysis of the hysteresis separating the data to build-up and decay periods. This is a demanding task when using field data. We decided to analyse the hysteresis on data from one particular day, Friday, 11.3.2022. After 15:00, the whole family gathered at home and started cleaning the house. This initiated excitement of the sensor signals suitable for separating decay and build-up periods. Figure 18 depicts the normalized data.

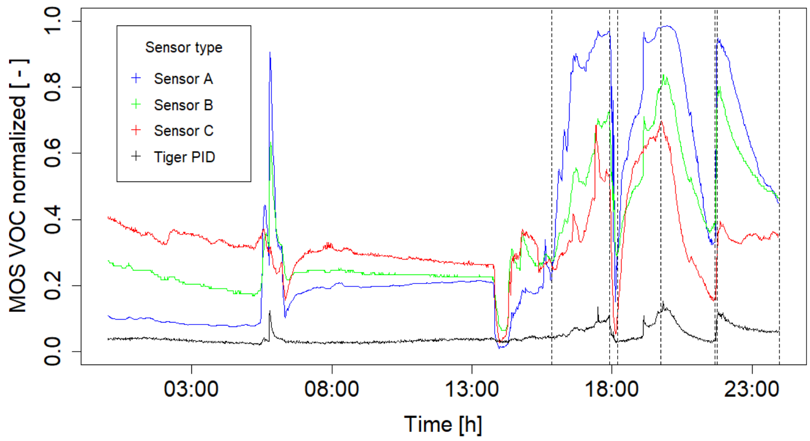

Figure 18 – Data used for evaluation of hysteresis; vertical dashed lines indicate selected build-up and decay periods

We illustrate the hysteresis in Figure 19. The determined values of the hysteresis were 0.123, 0.014, and 0.121 for sensors A, B, and C, respectively. We can see that the hysteresis was generally rather low, at 12.3%, 1.4%, and 12.1% of the measuring range. This was preferable. Sensors A and C had comparable hysteresis, while sensor B showed practically no hysteresis. Figure 19 also illustrates the relationship between the reference PID signal and sensor C. This time it seemed more consistent than when we considered a longer measurement period (Figure 17).

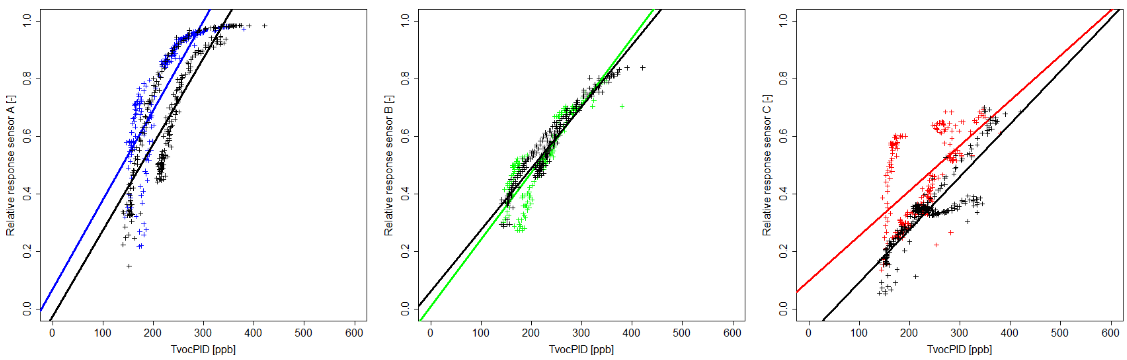

Figure 19 – Build-up and decay periods, and corresponding linear fits, the build-up is depicted in colour, the decay in black

With sensors A and B, the sensitivity we determined using a longer period (Figure 17) was comparable to that determined during one-day measurements. With sensor C, the sensitivity differed significantly. In the case of one-day measurements, the slope of the linear fits for sensor C was comparable to those of sensors A and B. This was not the case for a longer period; see Table 8. This indicates that sensor C had unstable behaviour when exposed to the pollution emitted in the kitchen. This is an issue, which cannot be fully explored within the current project. It seems that the character of the data obtained from the sensor C changed along its operation. More dedicated analysis would be needed to understand this phenomenon.

4.2 MOS VOC sensors for ventilation control – laboratory measurements

4.2.1 Test campaign 1

Figure 20a shows the unprocessed signal used to control the ventilation unit and the corresponding airflow. It can be seen from the graph that there were several fluctuations in the airflow (in the range of approx. 10 m^3/h) as the controller reacted to the peaks in the MOS VOC signal. It can also be seen from the graph that the strongest response occurred during the last part of the measuring scenario, namely hand disinfection. The use of hand sanitized emitted a high amount of ethanol.

The graphs presented in the Figure 20 demonstrate results from particular tests, where we investigated different values of the moving average time window (the k-value). Although we followed the pollution scenario described in Table 2, it can be seen from the figures that the signal from the MOS VOC sensor was not identical under all tests. During some of the tests, the concentration peaks were more flat. Despite this inaccuracy, it is visible that the signal processing algorithm reduced or completely removed small fluctuations in the signal, thus helping to prevent the regulator's oscillatory response. The effect of the post processing was very small for k value of 3 minutes. On the other hand, the high k values not only reduced the peaks of the signal, but also notably delayed the response of the air handling unit, which is not desirable. The main purpose of the control algorithm was to reduce unnecessary ventilation due to sharp peaks in the sensitive MOS VOC signal.

The Figure 21 displays duration curves for airflows and the signal of the MOS VOC sensor connected to the air handling unit. The duration curves demonstrate that there was no high spread in measured concentrations for the different tests, thus, the duration curves for the airflows were comparable. The airflow-related duration curves clearly demonstrate a specific reduction in airflow with an increased k value. When using the raw signal, the minimum airflow was used for about 52% of the time, and this value changed to 64% with k = 5 min and to 68% with k = 15 min. For the algorithm with variable k value, the percentage of time with minimum airflow was comparable to k = 5 min. However, the consequent approximately 32% of time, the variable k algorithm worked with in average 12.5% lower airflow. In the last part of the graph, the area with highest VOC concentrations, about 4% of time, the variable k algorithm worked with the highest airflows. The reason for this was that we designed the adaptive algorithm to increase the k value progressively all the way up to the highest levels of the MOS VOC signal. This does not seem to be a good strategy for sharp and large peaks caused, for example, by the emission of hand sanitizer. The high k value sustains the elevated airflow – note the plateau in the duration curves for k = 15 min and variable k in the Figure 21, respectively.

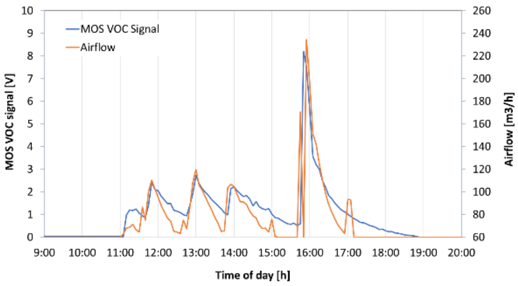

a) Unprocessed signal

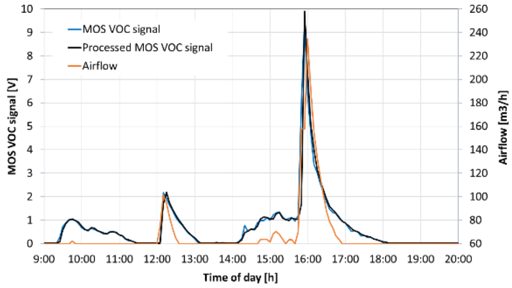

b) k-value = 3 min.

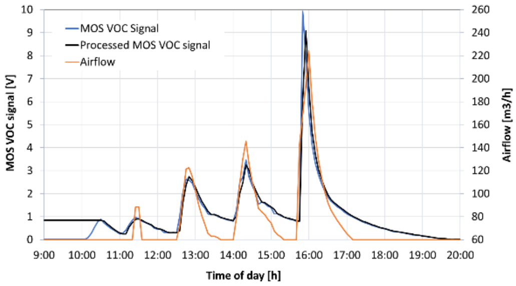

c) k-value = 5 min.

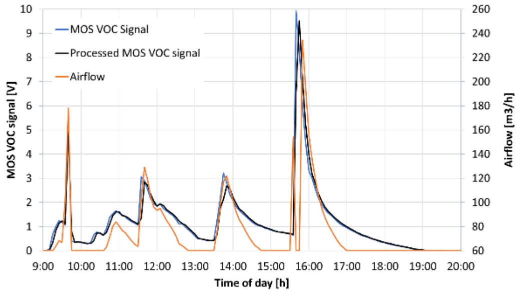

d) k-value = 10 min.

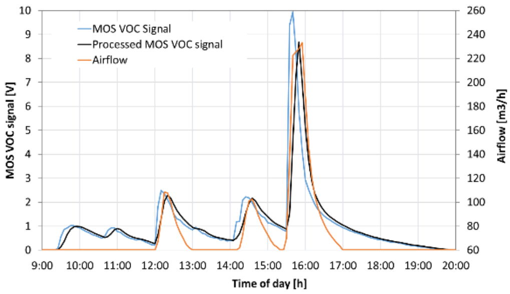

e) k-value = 15 min.

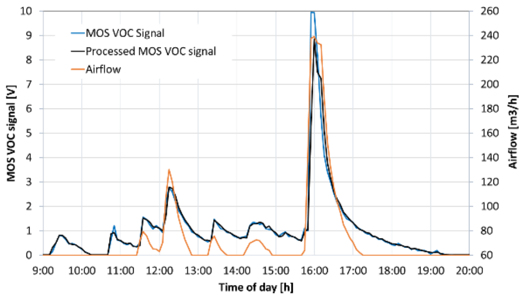

f) variable k-value

Figure 20 – Airflow control using unprocessed signal as well as different values of k parameter for moving average in the MOS VOC signal processing

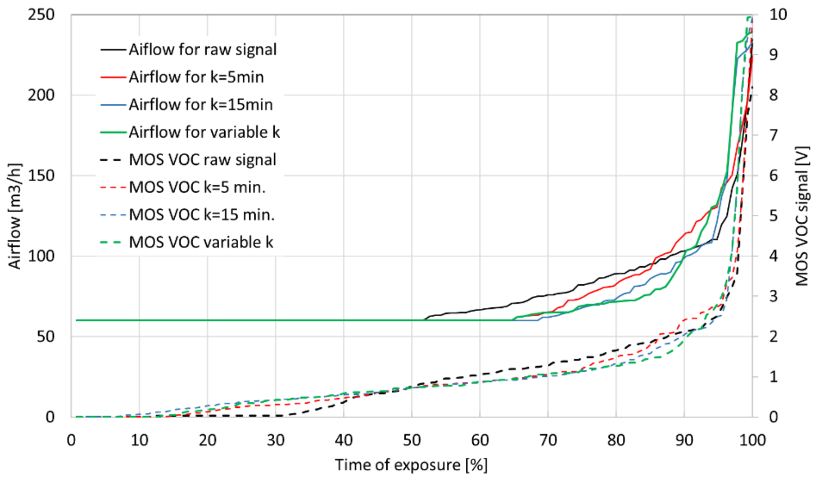

Figure 21 – Duration curves for airflow and MOS VOC signal measured by the sensor connected to the air handling unit

4.2.2 Test campaign 2

Air quality control by the air handling unit

Figure 22 shows the reactions of the commercially available IAQ control algorithm embedded in the utilized air handling unit. The unit was controlled according to its internal controller - “Automatic air quality control” (proprietary; no detailed information about the algorithm was available). Additionally, the PID signal is presented for comparison. The pollutant emission corresponded to the Pollution scenario 1 from Table 3. The figure shows that the MOS VOC sensor in the air handling unit could detect the human entry into the room, unlike the PID monitor. On the other hand, the PID reacted more strongly to the orange peeling (Exposure A). The sensors showed similar reactions with Exposure B and C (window cleaning and hand disinfection). It is important to note that the air handling unit worked with IAQ control only for the operating mode “Home” (see section 3.3.2), so the control signal did not drop below 5 V (to minimum airflow). The airflow at this level is rather high. Therefore, the emissions of human bioeffluents from the entering person did not increase the airflow.

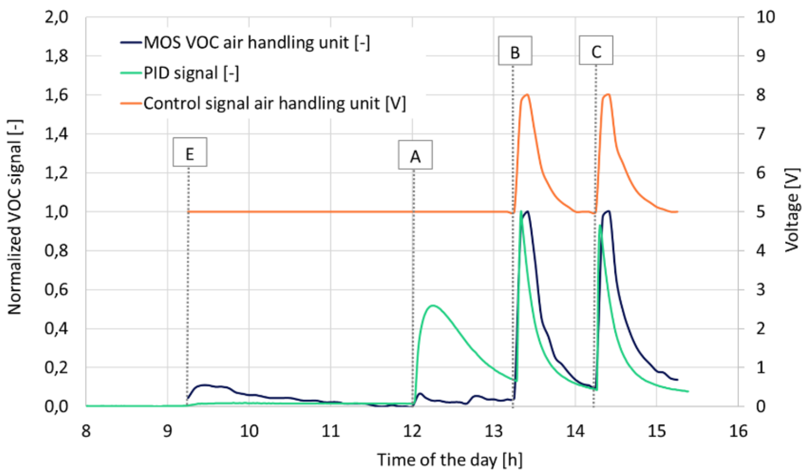

Figure 22 – Response to Pollution scenario 1 by commercial IAQ control by the MOS VOC sensor installed in the air handling unit; E – human enters the field laboratory, A, B & C – Exposure A, B and C respectively

Control by the algorithm developed in the project

Figure 23 shows the response of the external MOS VOC sensor controlled according to the moving average algorithm. The output signal ranges from 1-8 V as the unit was set to the “step less” operating mode. In this mode, the fan's rotation speed changed continuously between minimum and maximum values. The minimum value corresponded to the minimum in the control algorithm embedded in the unit (Figure 22). However, the minimum flow at that algorithm is indicated by 5 V control signal. Therefore there is a vertical shift in the control signal between the figures.

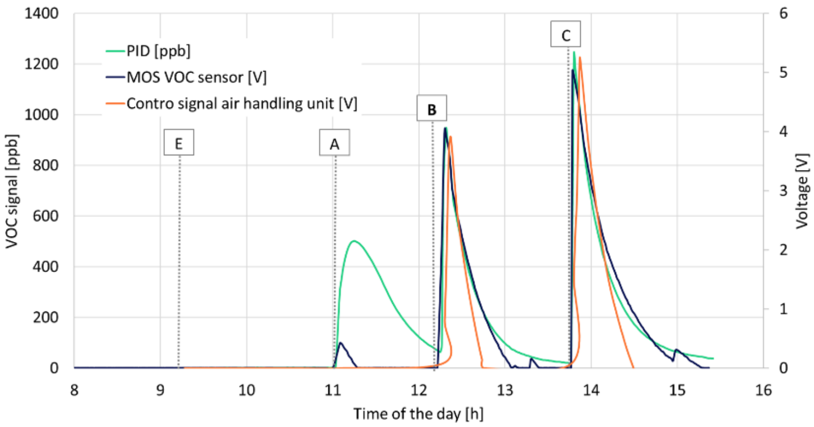

Figure 23 – Response to Pollution scenario 1 by the control algorithm developed in the project; E – human enters the field laboratory, A, B & C – Exposure A, B and C respectively

In Figure 23, we can see that neither the MOS VOC sensor nor the PID detected the human presence in the room. The PID once again showed a stronger response to orange peeling (Exposure A). Furthermore, as with the previous test, both sensors reacted similarly to exposures B and C. It is also visible, that the ventilation control signal did not respond to exposure A, as in the previous case. The control signal was slightly shifted to the right for exposures B and C, indicating delayed response. Otherwise, the signal closely followed the MOS VOC signal.
When comparing the control using the control algorithm developed within the project and the algorithm from the unit, we observe a similar behaviour.

Response of all investigated sensors

We conducted additional tests with the air handling unit being controlled by its air quality control algorithm. The Figure 24 shows the signals from all sensors used in the project.

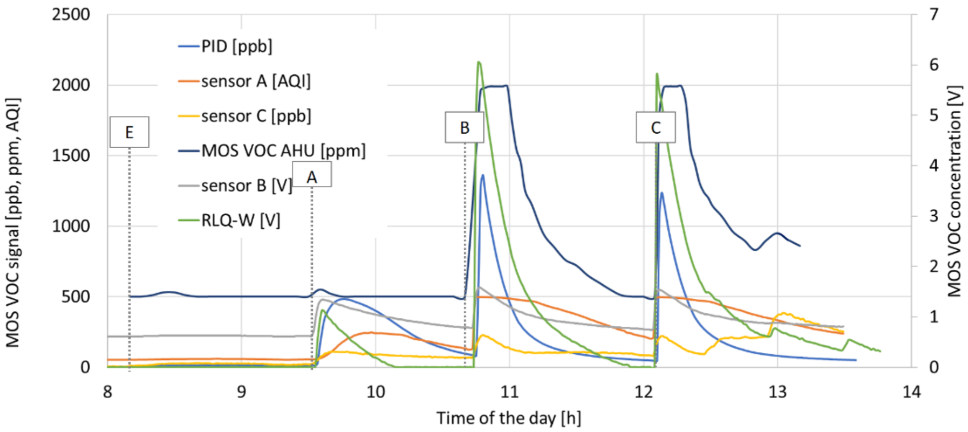

Figure 24 – Comparison of all investigated sensors in the field laboratory

The Figure 24 depicts the measured values by the respective sensors in their output units. It is clear from the figure, that the reaction of the sensors to a human entering the room was weak. Human bioeffluents from one person were not, at the used airflow, enough to trigger a notable response. The sensor from the air handling unit had a weakest reaction to the limonene emitted during orange pealing. The remaining sensors produced notable responses. At the same time, the character of the response was not the same for all of them. Sensor A reacted with a flat peak with a certain delay, sensor C had even milder reaction. The responses to stronger pollution events – window cleaning (B) and hand sanitizer (C) resulted in sharp peaks for sensor RLQ-W and the PID instrument, sensor A reached its maximum (500 points of an air quality index) and the signal stayed on high levels notably longer than for other sensors. A similar behaviour could be observed for the sensor in the air handling unit. The prolonged time with the signal at high values was most probably caused by these two sensors' internal data processing algorithm.

Exposure to evaporation of ethanol

On Figure 25 we can see results of the last conducted experiment. Exposure of the sensors to the emission of ethanol. We conducted two experimental sessions with this emission, but only data from one of the sessions are available due to the technical failure. Figure 25 clearly shows a saturation (sometimes also called poisoning) of the sensor A. Sensors B and RLQ-W reacted similarly, reaching their peak for approximately one hour and then decaying. On the other hand, the sensor C held its maximum value for a minimal duration and started the decay much earlier. We can observe a comparable behavior when relating to the results for the exposures A, B and C from the Table 3. Sensor A exhibited prolonged periods at peak values followed by slower decays. The signal from sensor B had also shallow decays in contrast to the remaining sensors, which were characterized by sharp peaks in the signal and immediate, rather steep decays.

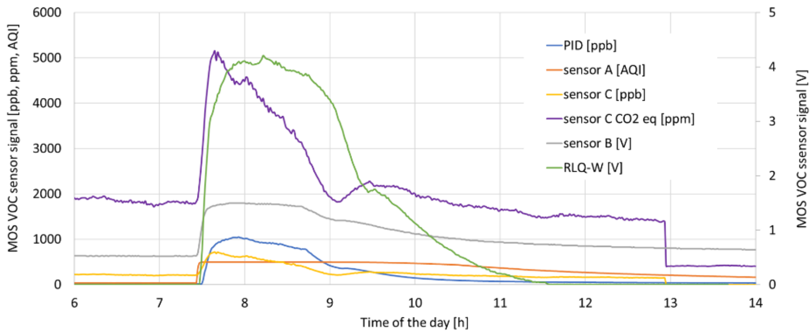

a)

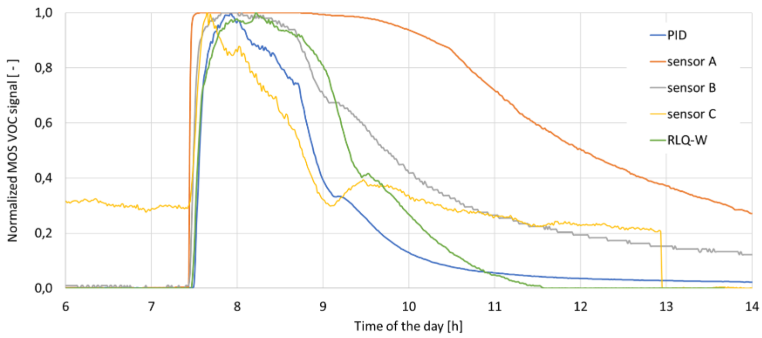

b)

Figure 25 – Exposure to emission of ethanol; a) absolute sensor signals, b) normalized sensor signals

4.3 Modelling energy consumption

Results from the simulations focus mainly on the key performance indicators related to energy consumption of heating and ventilation systems. Table 9 summarizes these results. Additionally, it presents also average daily mechanical airflow. We used mechanical exhaust airflow from the kitchen zone for this indicator. The air handling unit provided balanced airflow; therefore the similar airflow was supplied into the living room.

Table 9 – Simulation results regarding energy consumption and average airflow

Case	E_{heat} [kWh]	E_{el} [kWh]	Q_{day_avv}[L/s]
MVHR CAV	619	5.6	8.8
MVHR DCV	616	7.0	9.8
MVHR DCV_{VOC}	732	22.5	25.2
MVHR $DCV_{MA,\ k=15}$	758	30.0	27.4

Table 9 shows that MVHR CAV and MVHR DCV cases were comparable in terms of energy consumption for heating. This was caused by the fact that they both worked with the same minimum airflow, which was dictated by the Danish building regulations. The slightly higher electricity consumption for the DCV case was caused by the periods with increased airflow due to higher CO_2 concentration. The almost negligible difference shows that the minimum airflow was enough to keep the CO_2 concentration under 800 ppm most of the time. The MVHR DCV_{VOC} case represents the situation when the MOS VOC sensor replaced the CO_2 sensor. In this case, the system worked with clearly higher air flows. The energy consumption for heating and electricity consumption increased. The average daily mechanical airflow was also significantly higher. This behaviour was caused by the fact that CO_2 equivalent concentrations were generally higher in absolute values. Figure 26 compares CO_2 and CO_2 equivalent concentrations for the $MVHR_{CAV}$ case. It can be seen that the CO_2 equivalent signal was, in general, higher than actual CO_2 values. This is in line with observations done during the field measurements in the kitchen of the row house. Under the $MVHR_{CAV}$ (with daily kitchen exhaust boosts in the dinner time), the CO_2 concentration rarely exceeded 1000 ppm, while the CO_2 equivalent concentration was over 1000 ppm 81% of the time.

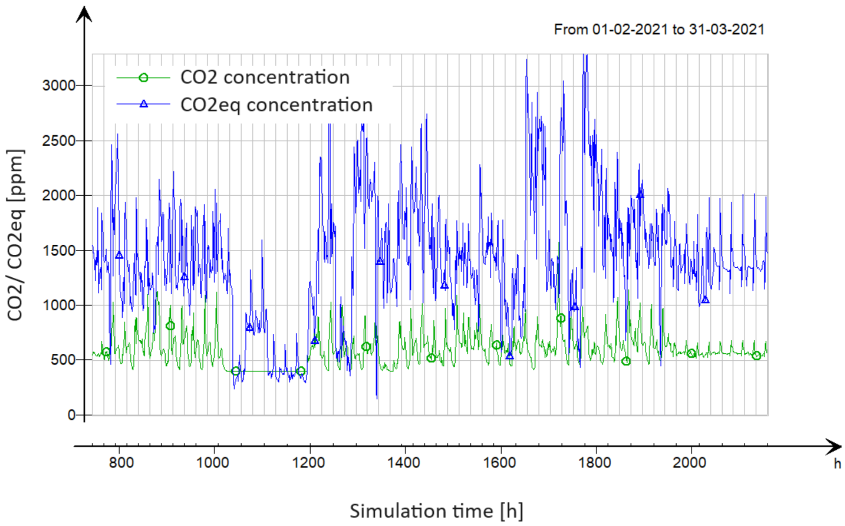

Figure 26 – Comparison of CO_2 and CO_2 equivalent signals for $MVHR_{CAV}$ simulation case for entire simulation period

Figure 27 illustrates the difference in airflows for the two types of demand control on a duration diagram. It is visible that the CO_2 based algorithm worked with minimum airflow for almost all the hours of the simulated period (> 1200). At the same time, the MOS VOC-based DCV stayed at minimum airflow for about 300 hours.

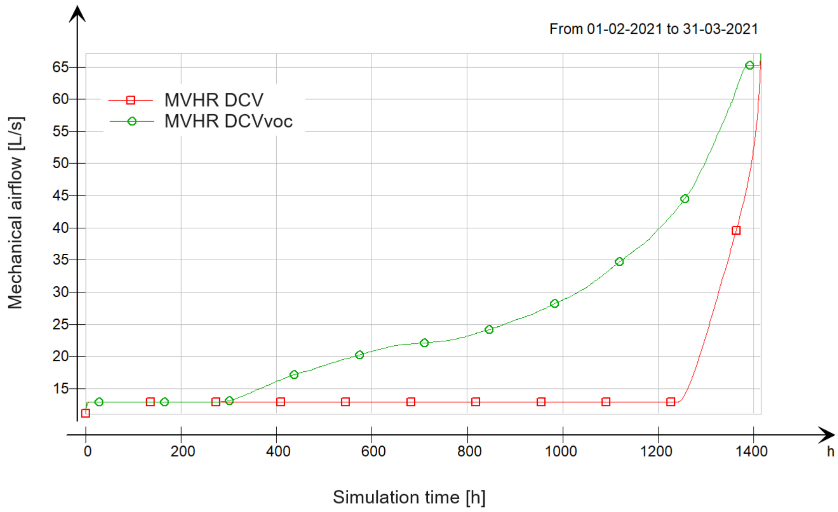

Figure 27 – Duration diagram comparing mechanical airflows for control by CO_2 and CO_2 equivalent signal

Figure 28 depicts one week of the hourly average concentrations of CO_2 and CO_2 equivalents in MVHR DCV and MVHR DCV$_{voc}$ cases, respectively. It can be seen that the algorithm using CO_2 equivalents keeps the set point at 800 ppm. On the other hand, the demand control using pure CO_2 did not need to increase the airflow as the CO_2 concentration mainly was far below the set point.

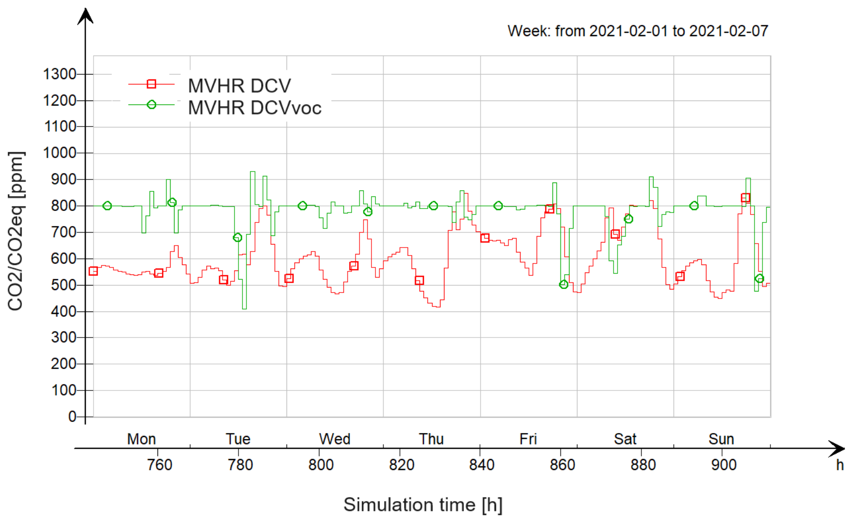

Figure 28 – Hourly average concentrations of CO_2 and CO_2 equivalent during one week simulated with MVHR DCV and MVHR DCV$_{voc}$ control, respectively

The results in Table 9 indicate that the algorithm with moving average further increased the energy consumption as well as used airflows. The difference to MVHR DCV$_{VOC}$ is not extensive, but it is undoubtedly a further increase. The Figure 29 documents the resulting airflows for the two control algorithms. It is visible that the algorithm utilizing the moving average uses the minimum airflow for a longer time. The control “waits” longer before increasing the airflow. Contrarily, the MVHR $DCV_{MA,\ k=15}$ algorithm works with higher airflows during the remaining time of the simulation. This is caused by the moving average extending the periods with high concentrations when the concentration peaks last longer. The change in the character of the duration curve from 800 h is apparent.

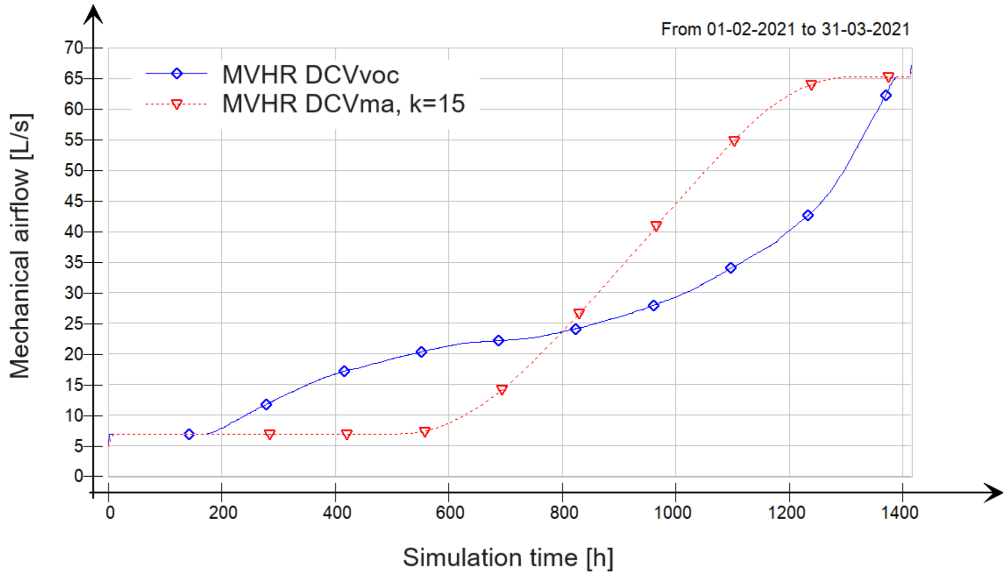

Figure 29 – Comparison of airflows for demand control algorithm using directly CO_2 equivalent values and the algorithm using 15 minutes moving average

It was impossible to simulate the algorithm with the adaptive k value of the moving average due to technical problems with the simulation model. It is clear from the simulations with k = 15 min that the moving average leads to even higher airflows than the direct use of the CO_2 equivalent signal.

5. Discussion

5.1 Measurements in real residential environment

Cross-correlation analysis

Cross-plots in Figure 16 visually indicate the relation between the signals from investigated sensors. We conducted a correlation analysis using the cross-correlation function (CCF) to describe this relation better. Figure 30 depicts the results corresponding to the period shown in Figure 14 (two weeks in October 2021). We determined the CCF for the MOS VOC sensors and the CO_2 and relative humidity signals. The CCF confirms the results based on the plots in Figure 16. The signals for sensors A and B were strongly correlated in the time lag zero with r = 0.8. The correlation between sensor C and sensors A and B was weak, with r = 0.3. There were also correlations in other time lags that reached over 95% confidence interval. None of these correlations had r > ±0.1. The latter results confirm the weak relationship between the sensor C and the remaining sensors. For all the sensors, there was a weak but significant correlation to relative humidity (r approx. 0.2) in higher time lags (time lag 25). This reveals the sensors' weak sensitivity to changes in relative humidity. Moreover, there was a considerable delay between the increases of the two signals. Considering the correlation between CO_2 and MOS VOC signals, the results were similar to those regarding relative humidity – a weak correlation in high time lags. The strong correlation (r = 0.6) between CO_2 and relative humidity at time lag zero suggested that they increased simultaneously. Such a common increase corresponds to the occupancy patterns in the house. As the occupants arrived from work and school, the CO_2 concentration increased.

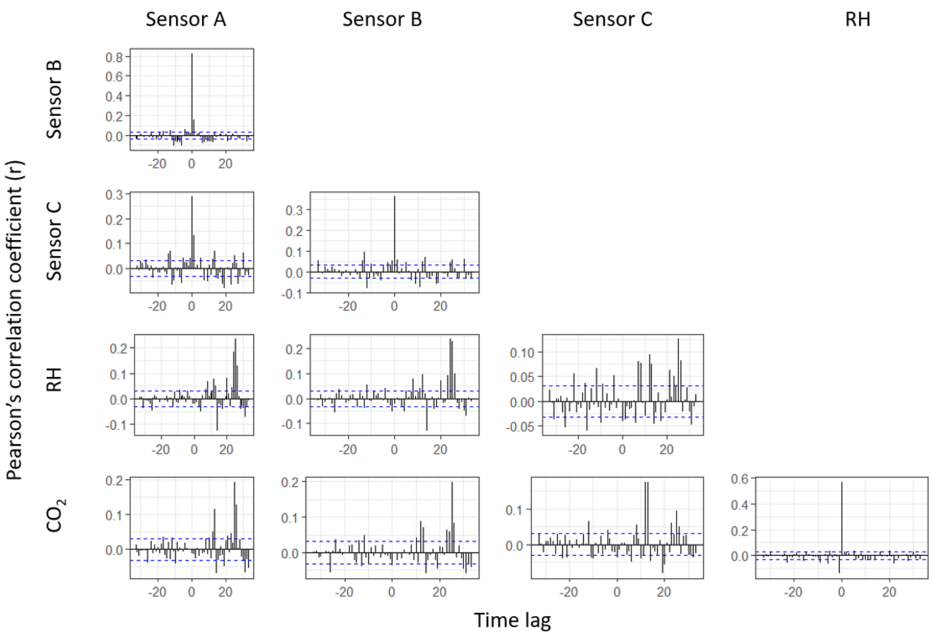

Figure 30 – A cross-correlation function (CCF) among investigated MOS VOC sensors, CO_2, and relative humidity measured in the kitchen; y-axis shows Pearson's correlation coefficient (*r*), blue dashed lines represent a 95% interval for *r*

CO_2 and CO_2 equivalent signals

Besides the $TVOC_{MOS}$ signal, sensor C also outputted a so-called CO_2 equivalent. Figure 31 compares CO_2 and CO_2 equivalent signals measured in the kitchen and bedroom. While in the bedroom, the CO_2 equivalent signal followed the CO_2 measurements rather closely. This was not the case in the kitchen. The possible explanation is that human bioeffluents were the primary source of pollution in the bedroom, while most other pollutants were emitted in the kitchen. The kitchen was directly connected to the living room, and the occupants, when not sleeping, spent most of their time there. The results indicate that when a stronger pollution event excited sensor C, its CO_2 equivalent signal had a tendency to drift from the CO_2 values. This can be a challenge concerning ventilation control. De Sutter et al. (2017) also observed differences in ventilation control when using CO_2 equivalent signals while keeping original set-point values in their study.

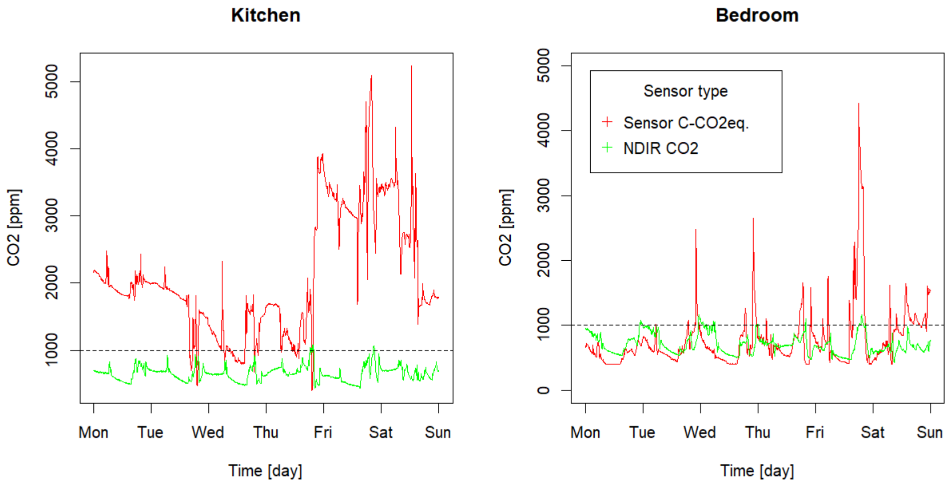

Figure 31 – CO_2 and CO_2 equivalent signal for measurements in the kitchen and bedroom; data from March 2022

From Figure 31, it is clear that applying the CO_2 equivalent signals would lead to increased ventilation. Using a set point of 1000 ppm for a system utilizing a MOS VOC sensor measuring CO_2 equivalents would lead to almost constantly increased airflow in the kitchen. It would be in great contrast to using the same value for a system utilizing an NDIR CO_2 sensor. On the other hand, in the bedroom, such a set point would lead to several periods with boosted airflow when using CO_2 equivalents, but generally, the control would be comparable to the one based on CO_2. De Sutter et al. (2017) observed similar behaviour and suggested several methods for signal processing to avoid “overventilation”. However, the question is whether such “overventilation” isn’t just the price one needs to pay for better IAQ. The fact that there is a disagreement between CO_2 and CO_2 equivalent signals, pointed out by several other authors (for example Moreno-Range et al. 2018) does not disqualify the MOS VOC based control. We can consider whether the fact that the MOS VOC signal is called “CO_2 equivalent” does not bring false expectations, namely, that it will agree with pure CO_2. Moreover, Demanega et al. (2021) pointed out notable differences in absolute values of the MOS VOC sensor signals, even though they did not deal with CO_2 equivalents.

Application of MOS VOC sensors for ventilation control

In our experiments and measurements, all tested sensors demonstrated the ability to react to pollution events in the house. The signal from sensor C seemed to be least correlated to the reference PID measurements in the kitchen. Moreover, the correlation between the signal from sensor C and the response of the other two investigated sensors was weak, too. Analysis using cross-correlation function-CCF revealed the similar results. While sensors A and B would yield comparable results, our data suggest that this would not be the case for sensor C when used for ventilation control. The most probable reason for such a difference is that the active layer of the sensor C was sensitive to different mixtures of VOCs. The results of Kolarik et al. (2023) similarly showed that depending on the type of exposure, there were differences between the studied sensors. Some were clustered together, indicating their response had similar patterns, while others were placed in different clusters. Thus, their response had dissimilar patterns. The authors estimated that there probably were different "driving" compounds for particular sensors. Kolarik et al. (2023) did not analyse CO_2 equivalent signals. However, the signal from four out of five tested MOS VOC sensors was clustered with the signal from the NDIR CO_2 sensor during exposure to human bioeffluents. In this case, humans were the only source of pollution in the test room. With the exposure to pollution from cleaning, two MOS VOC sensors showed different patterns. The results of our measurements are not directly comparable to those of Kolarik et al. (2023). However, considering both studies, it seems that MOS VOC sensors can detect occupancy in the same way as CO_2 sensors. At the same time, their signal weakly correlates to the actual CO_2 measurements unless humans represent the exclusive pollution source.

As discussed in the previous section, the difference in proportions of the absolute signals produced by MOS VOC sensors can challenge selecting the right set point. Laverge et al. 2015 discussed the challenge of establishing the set point value for a system utilizing CO_2 equivalent signal. The manufacturer of sensor A has approached the problem mentioned above by using the so-called "VOC Index." This measure, calculated continuously using the raw signal from the MOS VOC sensor, uses a proprietary algorithm that normalizes the signal using a time window of 24 hours. Figure 32 plots the sensor A signal for the kitchen and bedroom during the same period as in the Figure 31. This reveals the differences from the signal provided by sensor C as well as CO_2 concentrations measured by the NDIR sensor.

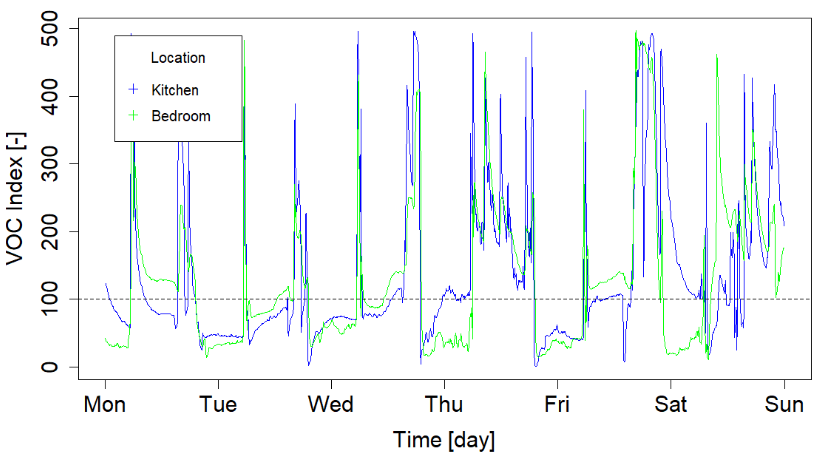

Figure 32 – VOC Index signal from Sensor A for measurements in the kitchen and bedroom; data from March 2022

The manufacturer assigns a value of 100 for the VOC Index as the average VOC concentration "intensity" (a typical IAQ). Intensity denotes that the MOS VOC sensor can only measure relative values, not absolute concentrations. With such an approach, the ventilation control could work with set points in the form of VOC Index values. As the VOC Index is related to the history of the signal in a particular room, systems that do not allow room-based airflow control should apply a decision algorithm. For example, the system should control always after the room with the highest VOC Index. Placing the sensor in the exhaust duct just before the air-handling unit would not provide the correct picture of the air pollution in particular rooms, as also elaborated by Abdul-Hamid et al. (2014). Nowadays, many commercially available MOS VOC sensors do not offer signal processing in a form similar to the VOC Index described above. Here, the designer of the particular control algorithm needs to provide such processing to ensure robust and stable control.

5.2 MOS VOC sensors for ventilation control – laboratory measurements

The experiments in the field laboratory showed that all tested sensors had comparable behaviour concerning the tested pollution events. Sensor A processed the raw signal into an air quality index, offering the possibility of dealing with the relative nature of the MOS VOC measurement. This feature also simplifies the definition of the set point values for the ventilation system. The air quality control algorithm in the air handling unit enables setting the set points for particular airflow levels (Travel, Away, Home, etc.) using the values of VOC concentration in ppm units. However, these units do not realistically relate to any actual pollutant. The same problem appears with other tested sensors, except sensor C, which has a CO_2 equivalent output. With sensors providing the output signal in concentration units (ppm, ppb) or an analogue signal (voltage), the set points should be established using different predefined pollution scenarios. The present project suggests such scenarios in Tables Table 2 and Table 3.

Based on our measurements, we consider the steep response of the MOS VOC sensors to sudden emissions to be the biggest challenge. These peaks, followed by rapid decays, trigger the ventilation system into short periods with maximum airflow. Sensor A, applying the signal processing, seemed to deal with this challenge; however, rather by “flattening” the decays end “shaving the peaks.” The peak in the sensor signal leads to a sudden boost in the ventilation airflow, which, most probably, does not influence the energy consumption of the ventilation on a long term basis, but can create unnecessary draught and noise and thus discomfort for the occupants. The control algorithm designed and tested in the project was based on the utilization of running mean of the MOS VOC signal, applying different averaging periods. The averaging period of 15 min and the variable averaging period had comparable performance. They reduced the peak airflow and, at the same time, sustained the high airflow for about 15 min. after the peak emission (Figure 20). This behaviour was comparable to the behaviour of sensor A. As seen from the Figure 21, the algorithm with variable averaging time and the one with k = 15 min led to the highest percentage of time with nominal airflow. However, it also resulted in more extended periods with prevailing high (maximum) airflow. Such behaviour ensures that when there is a high emission of pollutants, the ventilation airflow does not fall immediately with the MOS VOC sensor signal but remains high for several minutes to ensure the removal of pollutants. De Sutter et al. (2017) suggested several other methods for signal processing but did not demonstrate them practically, only by calculations. The current project couldn't test their strategies. Combining the algorithm with variable averaging period with the methods suggested by De Sutter et al. (2017) would be interesting for future work. Additionally, the algorithm developed within the project should be supplemented with a feature that eliminates the influence of the relative MOS VOC measurement. Thus, the running mean value of the sensor signal would not be used as a directly measured variable for the controller but rather to calculate an index, taking into account the relation of that value to the central tendency of the signal within an extended averaging period (for example 24 h).

PID measurements conducted in the field laboratory in parallel with the MOS VOC measurements showed rather fair agreement in terms of general trends in the obtained concentration patterns rather than absolute values. As shown in section 4.1 of this report, using the PID to establish sensor properties will probably not be necessary in practice. However, the PID measurements can serve as a suitable accompanying measurement when model pollution scenarios are tested.

5.3 Modelling energy consumption

We performed modelling of the ventilation system's performance controlled by MOS VOC sensor on a simplified model of the test house. Several difficulties are involved in modelling the performance of MOS VOC sensors in building simulation. For the first, most building performance simulation tools do not allow modeling emissions of volatile organic compounds. Tools like Contam (Dols and Polidoro 2020) can be utilized to model such emissions. However, they have limitations concerning modelling the ventilation systems, controls, and thermal environment. Recently, attempts have been made to connect the functionalities of building performance simulation tools with those that model VOC emissions (De Jonge and Laverge 2021). Such modelling was not possible within the framework of the present project but gave promising possibilities for future work.
The second challenge is the modelling of the MOS VOC sensor behaviour. Even if the simulation tool predicts the VOC emissions and corresponding concentrations, it has been shown in the field measurements of the present project, that the nature of the MOS VOC sensor signal does not necessarily correspond to such concentrations. Therefore, experimental evaluation of the MOS VOC sensor behaviour and determination of the grey box model representing its behaviour would be necessary. This approach has already been used to calibrate MOS VOC sensors, for example, Baur et al. (2021) or Chojer et al. (2020). Its disadvantage is that it requires precise, laboratory grade VOC measurement instrumentation. In the present project, we used data obtained in the test house under real life conditions and applied them in the simulation model. There are obviously many uncertainties related to such an approach. We measured the CO_2 and CO_2 equivalent concentrations under certain conditions in the test house, and we were not fully capable of recreating all these conditions in the numerical model. For example, real house infiltration was probably different from the model. Also, the air mixing in the real house and concentration dynamics for the pollutants differed from the simplified simulation model with only three zones. Despite all the uncertainties, the MOS VOC emission profiles and corresponding CO_2 equivalent concentrations provided a surrogate for the MOS VOC sensor signal, which could be used for ventilation control.

It is clear from the simulation results that the algorithm developed during the project would not be the best suitable for the ventilation control. Using the moving average decreases the concentration peaks, as shown during the field laboratory tests, but it would generally prolong the periods with higher concentrations. Figure 33 depicts the results of a simulation model, where we used the daily running mean CO_{2eq} concentration as a set point. Thus the set point was not fixed, but it followed the average concentration in the kitchen. This approach was similar to using sensor

A from the long-term measurements providing the IAQ index values and could represent an alternative to the initially developed algorithm. It is important to note that this strategy did not lead to a significant decrease in energy consumption or the average air flow concerning the MVHR DCV_{VOC} or MVHR $DCV_{MA,\ k=15}$ strategy. It just offered an alternative to a fixed set point, which, because of the nature of the MOS VOC sensors, does not seem to be appropriate.

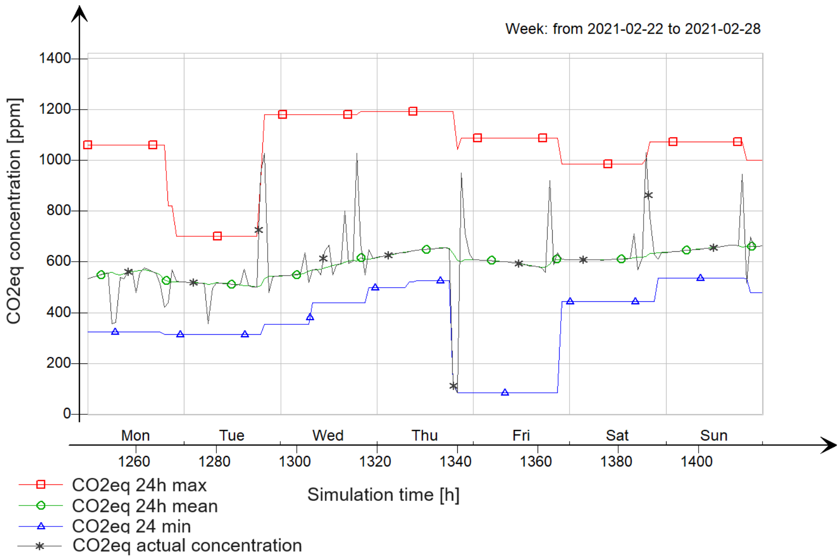

Figure 33 – MVHR ventilation controlled by 24 h average CO2 equivalent

It is not possible to judge the actual indoor air quality from building performance simulations. Different VOCs can trigger the MOS VOC signal, and elevated MOS VOC concentrations do not necessarily mean an immediate increase in health risk. However, because of this uncertainty, measurement identifying the key pollutants triggering the sensor's response should be known in advance (Kolarik et al. 2023).

5.4 General discussion remarks

Lastly, it is essential to mention that the research on MOS VOC sensors is progressing rapidly. Recent research on the calibration of MOS VOC sensors utilizes multiple regression models and deep learning algorithms (Schütze et al. 2017, Robin et al. 2021, Hong et al. 2023,). Such methods provide calibration models using multiple laboratory-grade measurements conducted parallel to the MOS VOC monitoring. These methods significantly improve the performance of MOS VOC sensors. In some cases, they enable selective monitoring of individual compounds due to the joint application of sensor measurement and deep learning algorithms, which are able to determine differences in sensor signals characteristic of individual compounds. Applying such advanced methods in residential ventilation will require a certain amount of time, but the directions in the current research are promising. These future trends, however, contrast with the reality of many ventilation practitioners and designers, who are confronted with ventilation systems equipped with MOS VOC sensors without substantial signal pre-processing ability.

Additionally, these practitioners usually cannot utilize laboratory-grade measurement instruments to determine sensor properties and characterize their response to different pollution events. Therefore, our work did not focus on calibration procedures but on simple methods for evaluating the performance of different MOS VOC sensors. The PID measuring instruments are generally available because they are used to characterize IAQ and detect emission hazards at workplaces and industrial buildings. Our work shows how the PID monitor can be utilized to cross-check the response of MOS VOC sensors under realistic and artificially created conditions. The observed response can consequently be utilized to determine the set point values or select the particular MOS VOC sensor.

Future work regarding MOS VOC sensors should focus on further development of suitable signal processing algorithms and the possibility of their practical use in residential ventilation systems. Follow-up projects should address the trade-off between energy efficiency and IAQ, considering the utilization of MOS VOC sensors. It is clear from the results of this project that the application of MOS VOC sensors does not primarily lead to a decrease in energy consumption. The opposite seems to be the case. Last but not least, in light of new work defining harm from indoor air pollutants by Morantes et al. (2023), combining MOS VOC sensors with sensors measuring particulate matter (especially PM 2.5) should receive attention in future research and practice related to residential ventilation control.

6. Conclusions

Measurements conducted in a real residential environment showed that all tested MOS VOC sensors detected air pollution emissions. However, not all the sensors had comparable sensitivity and produced comparable responses. For the two tested sensors, we can conclude that they would behave similarly when applied for control of a ventilation system. The third tested sensor presented a weak relationship concerning reference measurements. Moreover, the sensor signal did not correspond to the $TVOC_{PID}$ concentrations in isobutyl equivalents. This results indicate that the control engineer cannot expect the same behaviour from MOS VOC sensors by different manufacturers.

We used the PID monitor as a reference measurement and established sensor characteristics by comparing the MOS VOC sensors' output with the PID signal. This approach gave the possibility of comparing sensors' sensitivity and hysteresis.

We applied the Cross-correlation function to the measured data. This analysis revealed a weak correlation between the CO_2 equivalent signal by the MOS VOC sensor and pure CO_2 measurements. Significant discrepancies existed between the two signals in the kitchen, where the human bioeffluents were not the primary pollution source. The discrepancies in the bedroom seem smaller, but the correlation was also weak. The study results indicate that the characteristics of the MOS VOC sensors need to be appropriately considered in control algorithms. Moreover, the CO_2 equivalent signal does not seem to be a suitable surrogate for CO_2 concentration.

Recent developments in low-cost sensors measuring particulate matter (PM) bring a new perspective to using MOS VOC sensors. As PM represents by far the highest health risk for humans, one can expect that low-cost PM sensors will soon make their way into residential ventilation control. However, this does not necessarily disqualify the MOS VOC sensors. Future research should focus on controls that effectively combine those two.

We developed and tested the algorithm using a running mean with an adjustable time window (k) for processing the MOS VOC signal to control a small ventilation unit. The algorithm continuously adjusted the k value in response to the measured concentration. This adjustment reduced short peaks in the control signal and consequent short-term boosting of the ventilation airflow. However, the algorithm did not consider the relative nature of the MOS VOC measurement. We highly recommend this before its practical application.

Experiments in the field laboratory showed that all tested sensors had comparable behaviour under the tested pollution scenarios. During exposure to the emission of ethanol, which represents an extreme pollution event, one sensor showed signs of “poisoning”; however, the recovery time was no longer than two hours.

It was impossible to connect all tested sensors to the controlled and thus utilize them to control the air handling unit. We conducted parallel measurements, and their results indicate that all sensors reacted similarly to the pollution events. The differences in the character of their output signals would need to be considered during implementation with a concrete controller.

Modelling using a dynamic building performance simulation tool showed that utilization of CO_2 equivalent concentration for controlling the MVHR ventilation system led to higher heating energy consumption (by 16%) as well as extensive increase in fan electricity use (68%). This increase resulted from higher ventilation air flows used by the system due to higher absolute values of CO_2 equivalent concentrations. Utilization of moving average for the signal processing led to a slight but further increase in energy consumption. The moving average approach decreased the concentration peaks, but at the same time, it led to prolonged periods with higher concentration levels. The algorithm would need to be further optimized. In general, we can conclude, based on the results obtained, that the utilization of MOS VOC sensor signals would lead to increased ventilation compared to constant volume ventilation or ventilation controlled by pure CO_2 sensors.

Acknowledgements

We acknowledge the support from Bjarne Saxhof's Fond, Denmark.

We would like to thank Maria Justo Alonso, senior researcher at SINTEF, Norway, for her support and guidance regarding statistical analysis dealing with CCF.

We would like to thank Lars Kokholm Andersen and the team in the workshop and laboratories of DTU Construct for their support during the measurements.

Guest BSc students Josef Kovařík and Tomáš Celtovský from the Czech Technical University in Prague should be greatly acknowledged for their hard work and important contributions to the project.

References

Abdul-Hamid, A.; El-Zoubi, S.; Omid, S. (2014) Evaluation of set points for moisture supply and volatile organic compounds as controlling parameters for demand controlled ventilation in multifamily houses. *In Proceedings of the Indoor Air 2014*, Hong Kong, China, 7–12 July 2014.

Baur, T., Amann, J., Schultealbert, C., Schütze, A. (2021) Field Study of Metal Oxide Semiconductor Gas Sensors in Temperature Cycled Operation for Selective VOC Monitoring in Indoor Air. *Atmosphere*, 12, 647. https://doi.org/10.3390/atmos12050647

BR18 (2021) Bygningsreglementet. Social- og Boligstyrelsen. https://bygningsreglementet.dk/ (last visited July 2024)

Burdack-Freitag A, Rampf R, Mayer F, Breuer K (2009) Identification of anthropogenic volatile organic compounds correlating with bad indoor air quality. *In: Proceedings of the 9th International Conference and Exhibition Healthy Buildings 2009*, Syracuse, NY

Chojer, H., Branco, P.T.B.S., Martins, F.G., Alvim-Ferraz, M.C.M., Sousa, S.I.V. (2020) Development of low-cost indoor air quality monitoring devices: Recent advancements. *Science of The Total Environment*, 727. https://doi.org/10.1016/j.scitotenv.2020.138385

Demanega, I., Mujan, I., Singer, B. C., Anđelković, A. S., Babich, F., & Licina, D. (2021) Performance assessment of low-cost environmental monitors and single sensors under variable indoor air quality and thermal conditions. *Building and Environment*, 187. https://doi.org/10.1016/j.buildenv.2020.107415

De Jonge, K. and Laverge, J. (2021) Modeling dynamic behavior of volatile organic compounds in a zero energy building. *International Journal of Ventilation*, vol. 20, no. 3–4, pp. 193–203, doi: 10.1080/14733315.2020.1777012.

De Sutter, R., Pollet, I., Vens, A., Losfeld, F. and Laverge, J. (2017) TVOC concentrations measured in Belgium dwellings and their potential for DCV control. *In proceedings of 38th AIVC Conference*, Nottingham, UK

Dols, W. and Polidoro, B. (2020), CONTAM User Guide and Program Documentation Version 3.4, Technical Note (NIST TN), National Institute of Standards and Technology, Gaithersburg, MD, https://doi.org/10.6028/NIST.TN.1887r1 (last visited July 2024)

Durier, F., Carrié, R. Sherman, M. (2018) What is smart ventilation? *Ventilation Information Paper n. 38*, INVIE EEIG, Brussels, Belgium

DS/EN (2021) DS/EN 16798-1:2019 DK NA: 2021 Energy performance of buildings – ventilation for buildings – Part 1: Indoor environmental input parameters for design and assessment of energy performance of buildings addressing indoor air quality, thermal environment, lighting and acounstics – Module M1-6 – National Annex NA related to EN 16798-1. Danish Standards Association. Copenhagen, Denmark

Energistyrelsen (2024) Håndbog for energikonsulenter. https://www.hbemo.dk/ (last visited July 2024)

Equa (2024) IDA Indoor Climate and Energy. EQUA Simulation AB, Solna, Sweden

Fahlen P, Andersson H, Ruud S (1992) Sensor Tests, Demand Control Ventilation Systems, *SP Report ISBN 91-7848-331-331-X*, Swedish National Testing and Research Institute, Boras, Sweden

García, M. R., Spinazzé, A., Branco, P. T. B. S., Borghi, F., Villena, G., Cattaneo, A., Sousa, S. I. V. (2022) Review of low-cost sensors for indoor air quality: Features and applications. *Applied Spectroscopy Reviews*, 57(9–10), 747–779. https://doi.org/10.1080/05704928.2022.2085734

Giobertti Morantes, Benjamin Jones, Constanza Molina, and Max H. Sherman (2023) Harm from Residential Indoor Air Contaminants. *Environmental Science & Technology* 2024 58 (1), 242-257. doi: 10.1021/acs.est.3c07374

Guyot, G., Sherman, M. H., & Walker, I. S. (2018) Smart ventilation energy and indoor air quality performance in residential buildings: A review. *Energy and Buildings*, 165, 416-430 https://doi.org/10.1016/j.enbuild.2017.12.051

Herberger S, Herold M, Ulmer H, Burdack-Freitag A, Mayer F (2010) Detection of human effluents by a MOS gas sensor in correlation to VOC quantification by GC/MS. *Building and Environment*, 45, 2430-2439

Herberger S, Ulmer H (2012) Indoor Air Quality Monitoring Improving Air Quality Perception. *Clean-Soil Air Water*, 40 (6), 578-585

Hong, G-H., Le, T-C., Lin, G-Y., Cheng, H-W., Yu, J-Y., Dejchanchaiwong, R., Tekasakul, P., Tsai, C-J. (2023) Long-term field calibration of low-cost metal oxide VOC sensor: Meteorological and interference gas effects. *Atmospheric Environment*, 310, https://doi.org/10.1016/j.atmosenv.2023.119955

Justo Alonso, M., Wolf, S., Jørgensen, R. B., Madsen, H., & Mathisen, H. M. (2021). A methodology for the selection of pollutants for ensuring good indoor air quality using the de-trended cross-correlation function. *Building and Environment*, 209, pp. 108668

Kolarik, J. (2014) CO_2 Sensor versus Volatile Organic Compounds (VOC) sensor – analysis of field measurements and implications for Demand Controlled Ventilation. *In proceedings of Indoor Air 2014*, Hong-Kong, China

Kolarik, J., Lyng, N. L., & Laverge, J. (2018). Metal Oxide Semiconductor sensors to measure Volatile Organic Compounds for ventilation control. Report from the AIVC Webinar: "Using Metal Oxide Semiconductor (MOS) sensors to measure Volatile Organic Compounds (VOC) for ventilation control", www.aivc.org (last visited July 2024)

Kolarik, J., Lyng, N. L., Bossi, R., Li, R., Witterseh, T., Smith, K. M., & Wargocki, P. (2023). Application of Cluster Analysis to Examine the Performance of Low-Cost Volatile Organic Compound Sensors. *Buildings*, 13 (8), https://doi.org/10.3390/buildings13082070

Laverge, J.; Pollet, I.; Spruytte, S.; Losfeld, F.; Vens, A. (2015) VOC or CO2: Are They Interchangeable As Sensors for Demand Control? *In Proceedings of the Healthy Buildings Europe 2015*, Eindhoven, The Netherlands, 18–20 May 2015.

Madsen, H. (2007). *Time series analysis*. Chapman & Hall. https://doi.org/10.1201/9781420059687

Moreno-Rangel, A., Sharpe, T., Musau, F., McGill, G. (2018) Field evaluation of a low-cost indoor air quality monitor to quantify exposure to pollutants in residential environments, *J. Sens. Sens. Syst.*, 7, 373–388, https://doi.org/10.5194/jsss-7-373-2018

PINHEIRO, C.L., O. TARANTO a E. TOMAZ. (2018) Study of volatile organic compounds (VOCs) emitted by orange bagasse drying process. *Process Safety and Environmental Protection*,114, 16-24, ISSN 0957-5820.

Salthammer, T., (2022) TVOC – revisited. *Environment International*, 167, https://doi.org/10.1016/j.envint.2022.107440

Schütze, A.; Baur, T.; Leidinger, M.; Reimringer, W.; Jung, R.; Conrad, T.; Sauerwald, T. (2017) Highly Sensitive and Selective VOC Sensor Systems Based on Semiconductor Gas Sensors: How to? *Environments*, 4, 20, https://doi.org/10.3390/environments4010020

Sørensen, S.B., Kristensen, K. (2024) Low-cost sensor-based investigation of CO2 and volatile organic compounds in classrooms: Exploring dynamics, ventilation effects and perceived air quality relations. *Building and Environment*, 254, https://doi.org/10.1016/j.buildenv.2024.111369

Wang, P. G. et al. (2013) 2001 – 2010 Danish Design Reference Year. Reference Climate Dataset for Technical Dimensioning in Building, Construction and other Sectors. Technical Report 13-19. Danish Meteorological Institute, Copenhagen, Denmark

Won, D.Y., Schleibinger, H. (2011) Commercial IAQ Sensors and their Performance Requirements for Demand-Controlled Ventilation. *Report no. IRC-RR-323*, National Research Council Canada